# Part III

## Improving polymer functionality

# 11

# Nanostructuring polymers with cyclodextrins

A. E. TONELLI, North Carolina State University, USA

## 11.1 Introduction

For over a decade my colleagues and I, and several other research groups, have been forming crystalline inclusion compounds (ICs) between host cyclodextrins (CDs) and various guest polymers.[1–73] When guest polymers are threaded by host cyclodextrins (CDs) to form crystalline polymer-CD-ICs, the included polymer chains are highly extended and isolated from neighboring chains. This is a consequence of the stacking of the cyclic oligosaccharides, α-, β- or γ-CD containing six, seven, or eight glucose units, respectively, which produces continuous narrow channels with ~ 0.5–1.0 nm diameters, where the guest polymers are included and confined (see Fig. 11.1).[6]

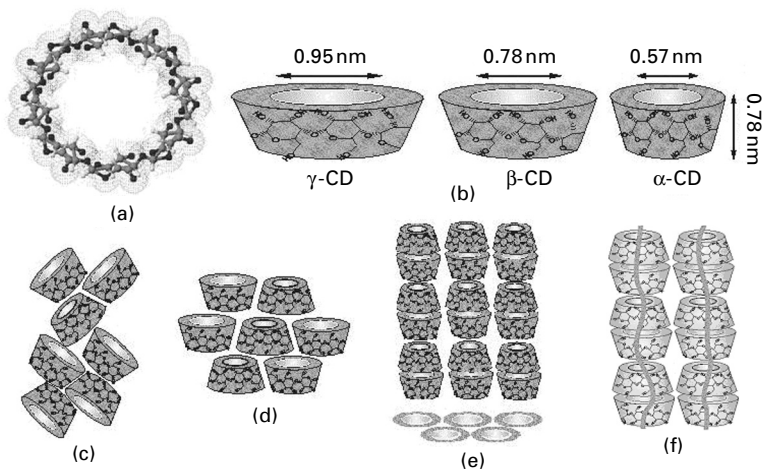


*11.1* (a) γ-CD chemical structure; (b) approximate dimensions of α-, β-, and γ-CDs; schematic representation of packing structures of (c) cage-type, (d) layer-type and (e) head-to-tail channel-type CD crystals; and (f) CD-IC channels containing included polymer guests.

My laboratory alone has formed polymer-CD-ICs with more than three dozen high molecular weight polymer guests,[1–52] covering a wide range of different chemical structures, including the fibroin protein from the *Bombyx mori* silkworm.[47] As a consequence, we have been attempting to understand why randomly coiling polymer chains in solution or the melt become threaded or thread into the nano-pores of dissolved or solid CDs, where they are highly extended and segregated from other polymer chains. The nano-threading of guest polymers into CDs to form ICs has added importance, because they can serve as model systems to probe various aspects of molecular recognition and supramolecular chemistry, which are so critical to life processes.

This chapter brings together and summarizes observations previously made in our laboratory that illuminate several important aspects of the nano-threading of polymers to form polymer-CD-ICs.[74] These include: (i) competitive CD threading of polymers with different chemical structures and molecular weights from their solutions containing suspended solid or dissolved CDs, (ii) the threading and insertion of undiluted liquid polymers into solid CDs, and (iii) suspension of polymer A or B-CD-IC crystals in a solution of polymer B or A and observation of the transfer of polymer B or A from solution to displace polymer A or B and form polymer B or A-CD-ICs, without dissolution of the polymer-CD-ICs. Comparison of these observations has enabled an assessment of the relative importance of several factors that have been previously suggested as being crucial in the formation of CD-ICs with both polymer and small-molecule guests and to the nano-threading of polymers in general.

The formation of and coalescence from polymer-CD-ICs are briefly described along with the methods used to characterize both the ICs and the coalesced guest polymers. Here the focus is on the structural organization of solid polymer samples coalesced from their CD-ICs, which are found to be quite distinct from solid polymer samples formed from their randomly coiling and entangled solutions and melts. The alteration and control of properties displayed by solid polymers coalesced from their CD-ICs are also discussed.

Polymers treated with and containing CDs, but that are only partially or not included at all by CDs, or that are covalently bound to CDs, are also considered, with particular emphasis placed on how their properties may be modified and controlled by their constituent CDs.

## 11.2 Formation and characterization of polymer–cyclodextrin–inclusion compounds

Formation of polymer-CD-ICs (see Fig. 11.1f and 11.2) begins with either the dissolution or suspension of CD cage-structure crystals (see Fig. 11.1c) or their conversion to channel- or columnar-structure crystals (see Fig. 11.1e) containing only water of hydration as a guest.[24] The formation of crystalline polymer-CD-ICs from solutions requires the combination of solutions

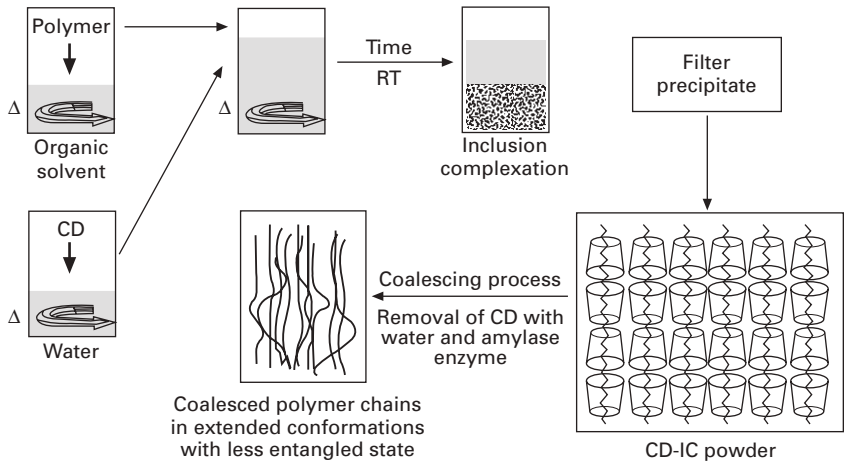


*11.2* Schematic representation of polymer-CD-IC formation, the coalescence process and the coalesced polymer.

containing the host CDs and the guest polymers, generally conducted with stirring at elevated temperatures,[48] followed by quiescent cooling, precipitation and filtration. On the other hand, suspension of either as-received cage-structure or columnar-structure CD crystals in polymer solutions[40] or in neat liquid polymers,[44, 45] can also produce polymer-CD-IC crystals.

By employing solutions containing two or more chemically distinct polymers during CD-IC formation, we may produce common CD-ICs that contain two or more guest polymers. Coalescence of the common guest polymers results in well-mixed polymer blends formed of two or more polymers that are generally observed to be immiscible.[17, 33, 39, 46] X-ray diffraction and/or solid-state $^{13}$C-NMR (nuclear magnetic resonance) observations of the resulting products can confirm the formation of channel-structure CDs and the presence of both the host CD and the guest polymer in the case of the latter technique. In addition, Fourier transform infrared (FTIR) and differential scanning calorimetry (DSC) observations enable the observation of the guest polymers and their inclusion in the channels of the host CDs, respectively. Dissolution of polymer-CD-ICs and observation by $^{1}$H-NMR can reveal their stoichiometries.

### 11.2.1 Coalescence of guest polymers from their cyclodextrin–inclusion compounds

As noted in Fig. 11.2, guest polymers may be recovered from their CD-ICs in the form of bulk solid samples by treating the polymer-CD-IC crystals with warm water or another CD solvent, which is a non-solvent for the guest

polymer, and or treatment with an amylase enzyme.[20] This process is termed coalescence and is usually conducted at temperatures below which the resultant consolidated guest polymers are immobile, i.e. below their glass-transition temperatures, $T_g$, to retain, as much as possible, their CD-processed and reorganized structures indicated in Fig. 11.2.

A wide variety of analytical techniques, such as wide-angle X-ray scattering (WAXS), FTIR, DSC, thermogravimetric analysis (TGA), solid-state NMR and mass spectrometry, are used to characterize the structures of polymer samples coalesced from their CD-IC crystals. The results of these observations are always compared with those obtained for as-received or as-synthesized, or melt or solution processed samples of the same polymers. In this manner, we attempt to assess process-dependent differences in their organization, such as morphologies, crystallinities and even the conformations adopted by their constituent polymer chains.

## 11.3 Properties of polymer–cyclodextrin–inclusion compounds

Liu and Guo[75] have summarized the interactions/driving forces that are often cited as playing significant roles in the formation of soluble small-molecule guest/host CD-ICs, and attempted to prioritize them in order of importance. Even though the formation is being discussed of solid crystalline columnar-structure CD-ICs containing polymer guests (see Fig. 11.1f and 11.2), where either both components are initially in solution or with solid CDs suspended in solutions of or in neat polymer guests, it is also useful to discuss and evaluate these same potential interactions/driving forces in connection with their formation. At the same time, because soluble and crystalline solid CD-ICs are most significantly distinguished by the regular packing of host CDs in the IC crystals, this distinction must also be considered in the present discussion.

### 11.3.1 Electrostatic interactions

The dipolar interactions between polar host CDs and included guests with permanent dipole moments are considered to affect at least the conformations and structures of soluble small-molecule guest/host CD-ICs.[75] Our observations[29] of the preference for inclusion of poly (ε-caprolactone) (PCL) over poly(L-lactic acid) (PLLA) chains in both dissolved and crystalline suspended α-CD (α-$CD_{CS}$), as well as the displacement of PLLA chains by PCL from PLLA-α-CD-ICs when suspended in PCL solution, indicate that dipole–dipole electrostatic interactions may not be critical to the formation of polymer-CD-ICs. If they were, then we might expect PLLA to be preferentially included in α-CD compared to PCL, because two PLLA repeat units and two ester group dipoles occupy each α-CD, while only single PCL

repeat units with a single identical ester group dipole are included in each α-CD.

Because both aliphatic polyesters likely adopt nearly fully extended all-*trans* conformations when included in their α-CD-ICs,[76, 77] the dipole moments in neighboring repeat units point in approximately opposite directions. This might cause partial cancellation of the net PLLA dipole moment in each α-CD, because two PLLA repeat units occupy each host α-CD, while only a single PCL ester group is included. Aside from this potential caveat, and because purely non-polar hydrocarbon polymers may be included in CDs,[42] *it is likely that dipolar electrostatic interactions do not play a major role* in the nano-threading and subsequent formation of polymer-CD-ICs.

### 11.3.2 van der Waals interactions

Liu and Guo[75] concluded that van der Waals interactions are a major driving force for the formation of soluble small-molecule guest/host CD-ICs. Because van der Waals interactions depend on molecular polarizabilities, and the two PLLA repeat units included in each α-CD are more polarizable than a single included PCL repeat unit, we tentatively suggest that *van der Waals interactions may not be important* in the formation of polymer-CD-ICs, because inclusion of PCL was observed to be preferred over that of PLLA.[29]

### 11.3.3 Hydrophobic interactions

Because PCL is less polar than PLLA, with an increased potential for hydrophobic interactions, we conclude that *hydrophobic interactions may be important* in the formation of polymer-CD-ICs, because, compared with PLLA, PCL is preferentially included by α-CD.[29] In addition, the observed[33, 46] competitive preference for the solution inclusion of bisphenol-A polycarbonate (PC) in γ-CD in the presence of poly(methyl methacrylate) and/or poly(vinyl acetate) further strengthens this conclusion, because PC is more hydrophobic than the other two polymers.

### 11.3.4 Hydrogen bonding

Once again the preference of PCL over PLLA inclusion[29] and the fact that all hydrocarbon polyolefins can form CD-ICs[42] imply that *hydrogen-bonding between included guest polymers and host CDs is not likely crucial* in the formation of polymer-CD-ICs.

### 11.3.5 Relief of conformational strain in cyclodextrins

Relief of conformational strain found in pure cage-structure CDs, which adopt asymmetric conformations,[75] cannot occur during polymer-CD-IC

formation from solutions, where CDs are dissolved, *may play a minor role* in the case of the formation of polymer-CD-ICs *through suspension of solid cage-structure CDs in polymer solutions*[40] *or in neat polymers*.[45]

### 11.3.6 Exclusion of cavity-bound, high-energy water

This is *not likely to be an important factor* for polymer-CD-ICs formed in solution. When forming polymer-CD-ICs by suspension of CDs in neat liquid polymers,[44, 45] or in their solutions,[40] however, some of the water bound in CD cavities must be displaced by polymer chains as they thread and are included in the suspended host CDs. In the case of poly (*N*-acylethylenimine) (PNAI),[40] inclusion from acetone solutions into both suspended cage and columnar structure γ-CDs, was prevented when using chloroform solutions. This strongly implies that the cavity water in CDs must have a suitable place to go when displaced by the inclusion of polymer guests, and likely is *important in the formation of polymer-CD-ICs by suspension of CDs in their solutions* and possibly also *in neat polymer liquids*. Drying cage structure α-CD before suspending into neat poly(ethylene glycol) (PEG) did not affect PEG inclusion,[44, 45] but this may have been the result of the compatibility between water and PEG.

To further assess whether or not exclusion of cavity-bound, high-energy water is an important factor when forming polymer-CD-ICs by suspension of CDs in neat liquid polymers or in their solutions, α-$CD_{CS}$ should be utilized. Vacuum drying of α-$CD_{CS}$ removes water of hydration residing in the α-CD channels, but does not result in changes in the columnar crystalline packing of α-CDs.[24] As a consequence, if air-dried and vacuum-dried α-$CD_{CS}$ are suspended in neat polymers or their solutions, we would expect the inclusion of polymers to be faster in the vacuum-dried α-$CD_{CS}$ if exclusion of cavity-bound, high-energy water is an important factor. Such experiments are currently in progress.

### 11.3.7 Crystalline packing of host cyclodextrins in solid cyclodextrin–inclusion compounds

When the α-CD-IC with guest propionic acid (PA) is formed either from solution or by suspending as-precipitated, air-dried α-$CD_{CS}$ in neat PA, a cage-structure PA-α-CD-IC results. Vacuum-drying α-$CD_{CS}$, which removes nearly two-thirds of the water contained by air-dried α-$CD_{CS}$, apparently stabilizes the columnar packing structure sufficiently to force PA to be included, without structural reversion to the generally preferred cage-structure PA-α-CD-IC.[24] Thus, interactions (presumably hydrogen-bonding) between neighboring α-CDs are increased by removal of interstitial hydration water upon vacuum-drying.

Columnar-structure CD-ICs are always formed with polymer guests, because of their long-chain nature, which requires their threading and inclusion by many CDs. This is consistent with the observation,[44, 45] that neat PEG oligomers are included in both as-received and vacuum-dried cage-structure α-CDs at the same rate and to the same quantity even though vacuum-dried cage-structure α-CDs have lost ~one-third of their hydration water,[78] presumably from their cavities, where they do not affect or stabilize the cage packing of α-CDs. However, when comparing the inclusion of both PEG oligomers,[44, 45] neat and in solution, and PNAI chains[40] in solution, into suspended cage- and columnar-structure α-CDs, the inclusion into α-$CD_{CS}$ is observed to be more facile. In the former/latter inclusion the packing structure of α-CDs is altered/unaltered, thereby illustrating the *importance of the crystalline packing of host CDs* in the formation of polymer-CD-ICs with solid CDs.

### 11.3.8 Nano-threading of polymers into solid cyclodextrins

Some all-hydrocarbon polyolefins in certain solutions have been observed to thread into γ-CDs and form polyolefin-γ-CD-ICs.[42] In concert with the large number of CD-ICs that have been formed with guest polymers having a wide variety of chemical structures, this strongly suggests that the *nano-threading of polymers is a general phenomenon* characteristic of their long-chain natures, or polymer physics, and not their detailed chemical structures, or polymer chemistry.[74]

We have observed: (i) the competitive CD threading of polymers with different chemical structures and molecular weights from their solutions containing suspended solid or dissolved CDs, (ii) the threading and insertion of undiluted liquid polymers into solid CDs, and (iii) suspension of polymer A or B-CD-IC crystals in a solution of polymer B or A and observation of the transfer of polymer B or A from solution to displace polymer A or B and form polymer B or A-CD-ICs, without dissolution of the polymer-CD-ICs. From these observations we have been able to illuminate several important aspects of the nano-threading of polymers. In particular, the value in observations of the inclusion of guest polymers, as well as small-molecule guests, into solid CDs suspended in their solutions and in neat guest liquids was made apparent, because interactions between host CDs, between CDs and solvents, and between guests and solvents, which complicate and make understanding the formation of polymer-CD-ICs difficult, are either eliminated or can be independently controlled in these experiments.[74]

Extension of the investigations summarized here should eventually permit a more complete answer to the question:

> 'Why do randomly coiling polymer chains in solution or the neat melt become threaded or thread into the nano-pores of dissolved or solid CDs

and zeolites, where they are highly extended and segregated from other polymer chains?'

However, we can currently conclude that *electrostatic*, *van der Waals* and *hydrogen-bonding* interactions and *relief of conformational strain in CDs are not important*, while *hydrophobic interactions, exclusion of high energy, cavity-bound water* and *crystalline packing of host CDs are important* in the formation of polymer-CD-ICs. Also the nano-threading of polymers appears to be a general phenomenon characteristic of their long-chain natures, or polymer physics, and not their detailed chemical structures, or polymer chemistry.[74]

## 11.4 Homo- and block copolymers coalesced from their cyclodextrin–inclusion compounds

When poly(ethylene terephthalate) (PET) was coalesced from its IC formed with γ-CD, it was observed to be significantly reorganized with respect to the as-received and solution and melt processed (normal) samples.[21, 32] For example, coalesced PET was found to have an FTIR spectrum that was distinct from those of normal PET samples, with much improved resolution. DSC observations of coalesced PET repeatedly evidence high-temperature crystallization, with resulting high crystalline contents, upon cooling rapidly from the melt, which is uncharacteristic of PETs that are generally slow to crystallize and can easily be quenched into a totally amorphous material. Furthermore, repeated DSC heating scans of coalesced PET fail to reveal a macroscopic glass-transition, and this was confirmed on a microscopic scale by measurement of temperature-dependent solid-state $^{13}$C-NMR-observed $^{1}$H spin-lattice relaxation times, $T_1\rho(^1\mathrm{H})$.[32]

Each of the behaviors unique to coalesced PET can be attributed to the g ± tg ∓ kink conformations assumed by its ethylene glycol fragments when included in the narrow channels of its γ-CD-IC, which are compared schematically in Fig. 11.3 (bottom) to the all-*trans* crystalline conformation (top) of PET. The kink conformations are nearly as extended as the crystalline, all-*trans* conformation, but they have a smaller cross-section, which explains their preferential inclusion in the narrow channels of its γ-CD-IC (see Fig. 11.1).[79] When coalesced from its γ-CD-IC the PET chains can readily and rapidly convert to the all-*trans* conformation through simple counter rotations about the —$CH_2$—O— bonds and therefore crystallize. Normal melts of PET consist of chains with predominantly g ± —$CH_2$—$CH_2$— bonds, which must be rotated to the *trans* conformation during crystallization. This conformational transition is difficult to accomplish without long-range movements of chain segments, consistent with the normally slow crystallization rate of PET. Furthermore, both solid-state FTIR and $^{13}$C-NMR observations

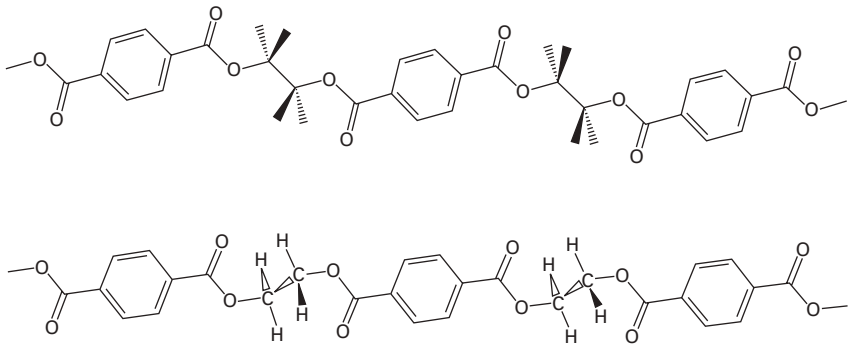

*11.3* Schematic of the crystalline all-*trans* (top) and γ-CD-included g ± tg ∓ (*gauche* ± *trans-gauche* kink ∓) (bottom) conformations of PET.

make clear that the kink conformations are largely retained by PET chains in the noncrystalline regions of the coalesced sample, and are also apparently substantially retained for a considerable period of time in the melt. This explains the ability of coalesced PET to be repeatedly and rapidly crystallized from its melt to high levels of crystallinity without application of high-temperature ($T > T_g$) annealing or solvent-induced crystallization.

The nanostructuring of PET by processing with γ-CD has important consequences for other macroscopic properties.[21, 32, 80] For example, compared with PET annealed at high temperature to achieve the same level of crystallinity as coalesced PET, the coalesced sample has a higher density and exhibits a reduced permeability to $CO_2$.[80] This implies a tighter packing of chains in the noncrystalline regions of coalesced PET.

### 11.4.1 PCL-b-PLLA di-block copolymer

When coalesced from its α-CD-IC, the structure and properties of the biodegradable-bioabsorbable di-block copolymer (PCL-b-PLLA) are found to be significantly different from the as-synthesized sample,[18, 20] as can be seen in Table 11.1. Note, for example, that both the levels of block phase segregation and crystallinity are substantially reduced in the coalesced di-block. This results in a much more rapid biodegradation of the coalesced di-block,[20] compared with the as-synthesized sample, which is critical to several of its potential applications.

The phase segregation and crystallinity of block copolymers may not be reduced only *via* the formation of and coalescence from their CD-ICs, as mentioned above for PCL-b-PLLA, but may actually be controlled through the formation of ICs using CDs which incorporate only some or all of the constituent blocks. For example, the phase segregation and crystallinity of

*Table 11.1* Thermal properties of as-synthesized and coalesced PCL-b-PLLA di-block copolymer (melting and crystallization temperatures $T_m$, $T_{cc}$, melting enthalpy $\Delta H_m$, and % crystallinity)

| Identity | $T_{m\ PCL}$ (°C) | $^{+}T_{cc\ PCL}$ (°C) | $\Delta H_{m\ PCL}$ (J/g) | $X_{c\ PCL}$ (%) | $T_{m\ PLLA}$ (°C) | $^{+}T_{cc\ PLLA}$ (°C) | $\Delta H_{m\ PLLA}$ (J/g) | $\chi_{c\ PLLA}$ (%) |
|---|---|---|---|---|---|---|---|---|
| As-synthesized di-block | 56.1 | 17.6 | 66.9 | 48 | 160 | 77.9 | 61.4 | 66 |
| Coalesced di-block | 63.7 | 29.3 | 35.0 | 25 | 164 | 93.9 | 12.5 | 13 |

*Table 11.2* Thermal properties (DSC) of various PCL-PPG-PCL tri-block copolymer samples[25]

| Identity | $T_{m\ PCL}$ (°C) | $\Delta H_{PCL}$ (J/g) | $\chi_{c\ PCL}$ (%) |
|---|---|---|---|
| As-synthesized copolymer | 57.3 | 58.6 | 56.5 |
| Sample coalesced from α-CD-copolymer IC | 63.8 | 76.8 | 74.1 |
| Sample coalesced from γ-CD-copolymer | 63.0 | 51.3 | 49.5 |

PCL blocks, $\chi_{c\text{-}PCL}$, in the tri-block copolymer PCL-poly(propylene glycol)-PCL (PCL-PPG-PCL) can be increased and decreased, respectively, compared to the as-synthesized sample, by employing α- and γ-CDs.[25] In the IC formed between PCL-PPG-PCL and α-CD only the PCL blocks are included in the α-CD channels, while the PPG blocks are excluded, which serves to segregate the PCL and PPG blocks. On the other hand, both PCL and PPG blocks are included in the IC channels formed with γ-CD, leading to an expected decrease in block segregation upon coalescence.

As can be observed in Table 11.2, both expectations are met. Phase segregation, as indicated by PCL block crystallinity, is enhanced compared with the as-synthesized sample when PCL-PPG-PCL is processed with α-CD, while processing with γ-CD enhances the mixing of crystallizable PCL and noncrystallizable PPG blocks.

## 11.5 Constrained polymerization in monomer–cyclodextrin–inclusion compounds

When the IC formed between γ-CD and styrene was suspended in water, which in this case did not result in dissolution of γ-CD, and a water-soluble free-radical initiator was added, the styrene was observed to polymerize to

polystyrene (PS),[37] without disruption of the channel structure of the host γ-CDs. Based on modeling the configurations and conformations of PS tetramers in cylindrical channels mimicking γ-CD,[9, 81] it was concluded that isotactic-PS (i-PS) could and syndiotactic-PS (s-PS) could not be accommodated in the γ-CD channels. Dissolution of the PSs obtained by the constrained polymerization of styrene in γ-CD channels and by the unconstrained homogeneous polymerization of styrene in an organic solvent and observation of their $^{13}$C-NMR spectra, did in fact reveal that the isotactic content of the PS obtained from styrene-γ-CD-IC was significantly greater than that of the homogeneously polymerized PS. Thus it appears that the microstructures of polymers may be controlled/altered by the spatially constrained polymerization of monomer-CD-ICs.

## 11.6 Coalescence of common polymer–cyclodextrin–inclusion compounds to achieve fine polymer blends

Though most polymers are found to be immiscible, it is possible to obtain well-mixed blends of any two or more polymers that can be dissolved in common solvents by processing with CDs.[39] This is achieved by first making a common CD-IC containing the polymers to be blended and coalescing them subsequently into a solid blend sample. Blending polymers by processing their common CD-ICs will be illustrated with the immiscible pair of biodegradable/bioabsorbable polyesters PCL and PLLA.[10]

Figure 11.4 compares the X-ray diffractograms of pure PCL and PLLA and their blends obtained by casting from their dioxane solution and by the hot water coalescence from their common IC with α-CD. Note that diffraction peaks from both PCL and PLLA crystals are prominent in the solution-cast blend (Fig. 11.4c), indicating a highly phase-separated morphology. On the other hand, in Fig. 11.4d the diffractogram of the PCL/PLLA blend coalesced from their common α-CD-IC, no diffraction peaks are observed for PCl crystals and only very weak peaks are observable for PLLA crystals. In fact, from DSC observation of the coalesced PCL/PLLA blend, it is estimated that no PCL crystals are present, and that only 5% of the PLLA is crystalline. Clearly then, the coalesced PCL/PLLA blend appears to be nearly totally amorphous and presumably well-mixed.

Two-dimensional solid-state spin-diffusion Hetcor NMR experiments revealed[82] that the coalesced PCL/PLLA blend was intimately mixed. The average minimum dimension for the amorphous coalesced PCL/PLLA blend was 4.9 nm, versus 7.4 nm for the amorphous regions of the semicrystalline PCL/PLLA blend prepared by dissolution in dioxane**.** The former dimension is comparable to the 4–5 nm radii of gyration for the particular PLLA and PCL polymers used, indicative of molecular level mixing in the coalesced

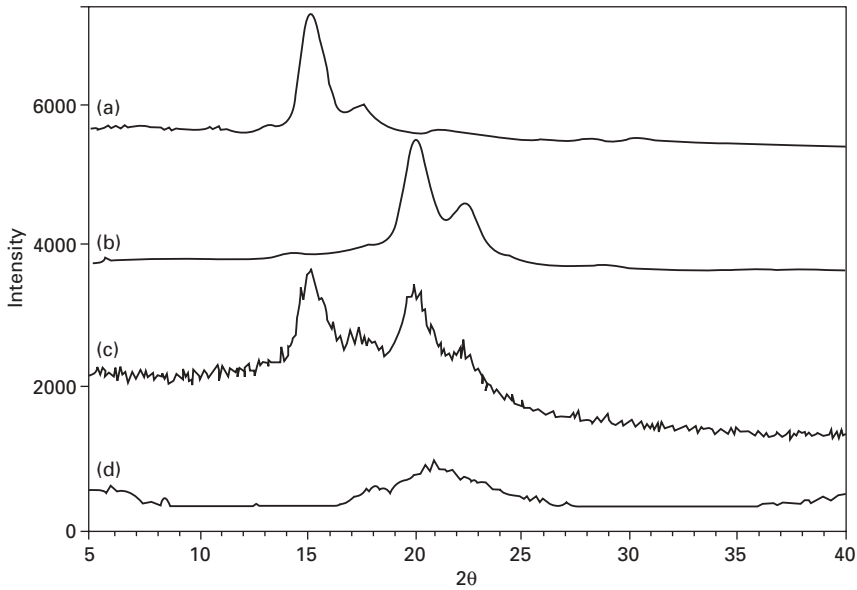


*11.4* X-ray diffractograms of pure PCL (a) and PLLA (b) and PCL/PLLA blends obtained by casting from dioxane solution (c) and hot water coalescence from PCL/PLLA-α-CD-IC (d).[10]

blend. Individual spin-diffusion coefficients, ***D***, for PLLA and PCL chains in the blends were calculated based on direct experimental measurement of the polymers in the blend. The magnitude of ***D*** was found to decrease by a factor of two for PLLA chains in the coalesced blend compared to pure PLLA, corroborating further the molecular mixing of PCL and PLLA chains in their coalesced blend. It is important to stress that blending polymers by coalescing their common CD-ICs is the only currently known method to achieve intimate solid-state mixing of normally incompatible polymers.

## 11.7 Temporal and thermal stabilities of polymers nanostructured with cyclodextrins

In general we have observed that homopolymer, block copolymers and polymer blends nanostructured by processing with CDs retain their unique solid-state organizations for considerable periods of time even at temperatures exceeding their $T_g$ and $T_m$ values, where their chains are potentially mobile. For example, PET coalesced from its IC with γ-CD continues to be rapidly crystallizable upon cooling from its melt, even after spending 2 h at ~300 °C.[21, 32] The PCL-b-PLLA di-block copolymer coalesced from its IC with α-CD remains more homogeneous, amorphous, and less phase segregated than an as-

synthesized sample even after it is heated above the $T_m$ of PLLA and then cooled from the melt.[18] In fact the intimately mixed PCL/PLLA blend made by coalescence of PCL and PLLA from their common IC with α-CD remains well mixed and does not phase separate even after being heated for several hours at 200 °C, well above the melting temperatures of both polyesters.[10]

The thermal and temporal stabilities of polymers nanostructured with CDs suggests that they may be melt-processed under normal conditions and still substantially retain their unique solid-state organizations, which should result in fibers, films and molded articles with distinct and possibly improved properties

## 11.8 Cyclodextrin-modified polymers

The behaviors and properties of polymers may also be modified with CDs and additive-CD-ICs. Because CD-ICs formed with small-molecule additives, such as antibacterials and flame retardants, are stable to temperatures beyond 250 °C, they may be compounded intact into many molten polymers. In this manner antibacterial[83] and flame-retardant[84] polymer fibers and films have been achieved.

Uncomplexed CDs may also be used to modify polymers. For example, when aqueous solutions of poly(vinyl alcohol) (PVA) are subjected to freezing/thawing cycles they produce hydrogels. When small quantities of γ-CD are added to the aqueous PVA before freezing and thawing, the resultant hydrogels are softer (lower modulus) and are more swellable then when prepared without γ-CD.[43] This behavior has been attributed to the partial threading of γ-CD by PVA chains, thereby reducing the number of microcrystalline cross-links subsequently formed between PVA chains during cyclic freezing/thawing.

The solution viscosity of the hydrophobically modified, alkali-soluble emulsion (HASE) associative polymer described in Fig. 11.5 can be controlled by the addition of α- and β-CDs.[30] CDs with their hydrophobic inner cores interact with the pendant macromonomeric segments of the associative HASE copolymer containing hydrophobic end groups and reduce their interchain hydrophobic interactions, leading to a reduction in solution viscosity and dynamic moduli by several orders of magnitude. The effect of CDs on the solution rheology of HASE copolymers is clearly demonstrated in Fig. 11.6, where the steady shear viscosities of aqueous HASE copolymer solutions are observed to be reduced ~a thousand-fold upon the introduction of α- and β-CDs. Furthermore, the reduction in polymer viscoelasticity in the presence of CD is reversibly recovered upon subsequent addition of different non-ionic surfactants that have a higher propensity to complex with the CDs than the hydrophobic macromonomer segments of the HASE copolymer.

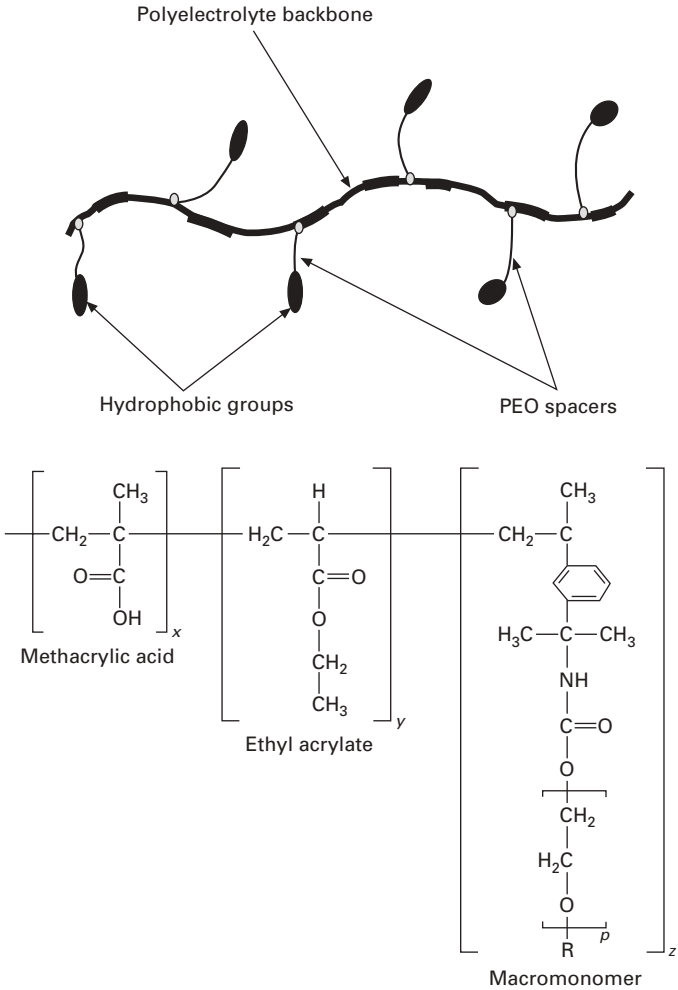


*11.5* Schematic representation of an HASE associative polymer and the molecular constitution of the HASE polymer used in this study.[30] R refers to the $C_{22}H_{45}$ hydrophobe, $p$ = 40, and $x/y/z$ = 43.6/56.2/0.20 by mole.

## 11.9 Polymers with covalently bonded cyclodextrins

Recently several reports of covalently bonding CDs to pre-synthesized polymers[85] and the synthesis of polymers incorporating CDs[86] have been published. The reactive Cl atom on monochlorotriazinyl-β-CD (CDMCT) can react with nucleophilic groups, such as the –OH groups on cellulose to permit grafting of CDMCT on cotton.[85] When cotton fabric grafted with CDMCT was immersed in solutions containing insecticides or insect repellents,

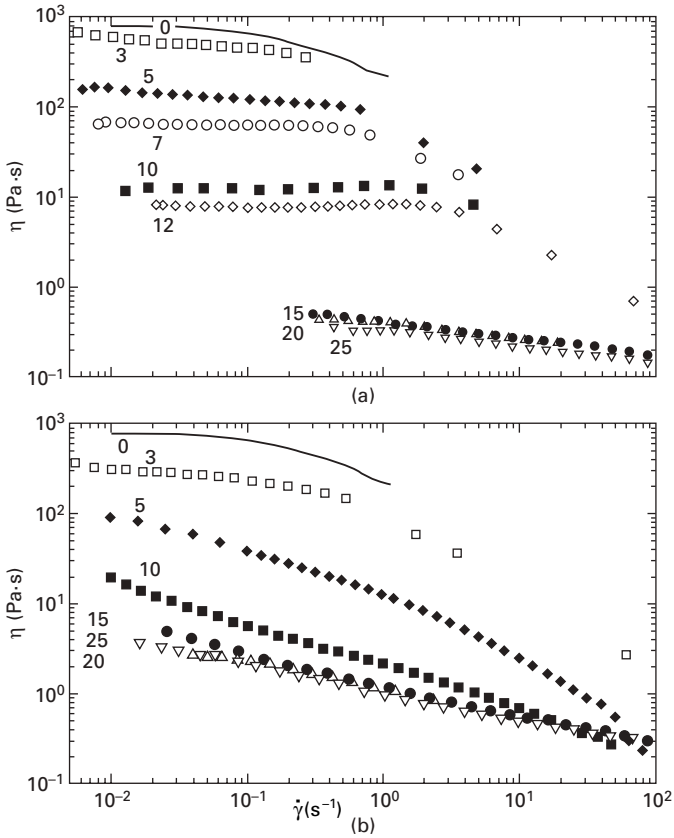


*11.6* Effects of addition of (a) α-CD and (b) β-CD on the steady shear viscosity of HASE associative polymer solutions.[30] Numbers correspond to the moles of cyclodextrin per moles of hydrophobe.

these active additives were complexed with the grafted CDMCTs, thus rendering the cotton fabric insecticidal or insect repellant.

Nylon-6,10 containing covalently bonded methyl-β-CDs (MBCD) was produced *via* interfacial polymerization of hexamethylene diamine in water and sebacoyl chloride plus MBCD pre-reacted with sebacoyl chloride in xylenes.[86] The MBCD–nylon-6,10 fibers drawn from the bi-layer interface were generally cross-linked due to the large number of –OH groups on MBCD, though cross-linking could be controlled by adjusting the ratio of MBCD pre-reacted with sebacoyl chloride to unreacted sebacoyl chloride.

When placed in a dye bath containing Acid Blue 29, the MBCD–nylon-6,10 fibers were observed to dye faster and absorb more dye than pure nylon-6,10 fibers. Apparently a portion of Acid Blue 29 dye enters the MBCD cavity and forms an Acid Blue 29-MBCD inclusion complex.

## 11.10 Conclusions

By way of the many examples discussed above, it should be clear that solid polymers may be effectively nanostructured by processing with CDs. Polymer solutions and gels may also be modified/controlled with CDs, and various functionalities may be delivered to them in the form of additive-CD-ICs. Finally, CDs may be covalently incorporated into polymers to provide them with permanent capabilities to bind and/or release a host of active agents.

## 11.11 References


1. Huang, L., Vasanthan, N., Tonelli, A. E., *J. Appl. Polym. Sci*., **64**, 281, 1997.
2. Tonelli, A. E., *Polymer Int*., **43**, 295, 1997.
3. Huang, L., Allen, E. J., Tonelli, A. E., *Recent Research Developments in Macromolecular Research*, S. G. Pandalai, Ed., Research Signpost, Trivandrum, India, 1997, Vol. 2, p. 175.
4. Huang, L., Allen, E., Tonelli, A. E., *Polymer*, **39**, 4857, 1998.
5. Huang, L., Tonelli, A. E., ACS Symposium Series # 728, *Intelligent Materials for Controlled Release Technologies*, S. M. Dinh, J. D. DeNuzzio and A. R. Comfort, Eds., ACS, Washington, DC, 1999, Chapter 10.
6. Huang, L., Tonelli, A. E., *J. Macromol. Science, Revs. Macromol. Chem. and Phys.,C* **38**(4), 781, 1998.
7. Huang, L., Allen, E., Tonelli, A. E., *Polymer*, **40**, 3211, 1999.
8. Lu, J., Shin, I. D., Nojima, S., Tonelli, A. E., *Polymer*, **41**, 5871, 2000.
9. Rusa, C. C., Tonelli, A. E., *Macromolecules*, **33**, 1813, 2000.
10. Rusa, C. C., Tonelli, A. E., *Macromolecules*, **33**, 5321, 2000.
11. Huang, L., Gerber, M., Taylor, H., Lu, J., Tapaszi, E., Wutkowski, M., Hill, M., Nunalee, F. N., Harvey, A., Rusa, C. C., Porbeni, F., Edeki, E., Tonelli, A. E., ACS Symposium Series # 790, *Film Formation in Coatings: Mechanisms, Properties, and Morphology*, T. Provder and M. Urban, Eds., Am. Chem. Soc., Washington, DC, 2001, Chapter. 14.
12. Lu, J., Mirau, P. A., Rusa, C. C., Tonelli, A. E., *Cyclodextrin: From Basic Research to Market, Proceedings of the 10th International Cyclodextrin Symposium* (CD-2000), May 21–24, 2000, Ann Arbor, MI., J. Szejtli, Ed., Mira Digital Publ. (314-776-6666), 2001.
13. Rusa, C. C., Lu., J., Huang, L., Tonelli, A. E., *Cyclodextrin: From Basic Research to Market, Proceedings of the 10th International Cyclodextrin Symposium* (CD-2000), May 21–24, 2000, Ann Arbor, MI., J. Szejtli, Ed., Mira Digital Publ. (314-776-6666), 2001.
14. Porbeni, F. E., Edeki, E. M., Shin, I. D., Tonelli, A. E., *Polymer*, **42**(16), 6907, 2001.
15. Rusa, C. C., Luca, C., Tonelli, A. E., *Macromolecules*, **34**, 1318, 2001.
16. Lu, J., Mirau, P. A., Shin, I. D., Nojima, S., Tonelli, A. E., *Macromol. Chem. Phys*., **203**, 71, 2001.
17. Wei, M., Tonelli, A. E., *Macromolecules*, **34**, 4061, 2001.
18. Shuai, X. Porbeni, F. E. Wei, M. Shin, I. D. Tonelli, A. E. *Macromolecules*, **34**, 7355, 2001.
19. Huang, L., Gerber, M., Taylor, H., Lu, J., Tapazsi, E., Wutkowski, M., Hill, M.,

Harvey, A., Rusa, C. C., Wei, M., Porbeni, F. E., Lewis, C. S., Tonelli, A. E., *Macromol.Chem., Macromol. Sympos*., **176**, 129, 2001.
20. Shuai, X., Wei, M., Porbeni, F. E., Bullions, T. A., Tonelli, A. E., *Biomacromolecules*, 3, **201**, 2002.
21. Bullions, T. A., Wei, M., Porbeni, F. E., Gerber, M. J., Peet, J., Balik, M., White, J. L., Tonelli, A. E., *J. Polym. Sci., Polym. Phys. Ed*., **40**, 992, 2002.
22. Shuai, X., Porbeni, F. E., Wei, M., Bullions, T. A., Tonelli, A. E., *Macromolecules*, **35**, 3126, 2002.
23. Wei, M., Davis, W., Urban, B., Song, Y., Porbeni, F. E., Wang, X., White, J. L., Balik, C. M., Rusa, C. C., Fox, J., Tonelli, A. E., *Macromolecules*, **35**, 8039, 2002.
24. Rusa, C. C., Bullions, T A., Fox, J., Porbeni, F. E., Wang, X. Tonelli, A. E. *Langmuir*, **18**, 10016, 2002.
25. Shuai, X., Porbeni, F. E., Wei, M., Bullions, T. A., Tonelli, A. E., *Macromolecules*, **35**, 2401, 2002.
26. Shuai, X., Porbeni, F. E., Wei, M., Bullions, T. A., Tonelli, A. E., *Macromolecules*, **35**, 3778, 2002.
27. Wei, M., Shuai, X., Tonelli, A. E., *Biomacromolecules*, **4**, 783, 2003.
28. Bullions, T. A., Edeki, E. M., Porbeni, F. E., Wei, M., Shuai, X., Tonelli, A. E., *J. Polym. Sci., Polym. Phys. Ed*., **41**, 139, 2003.
29. Rusa, C. C., Fox, J., Tonelli, A. E. *Macromolecules*, **36**, 2742, 2003.
30. Abdala, A. A., Khan, S., Tonelli, A. E., *Macromolecules*, **36**, 7833, 2003.
31. Tonelli, A. E., *Macromol.Chem., Macromol. Sympos*., **203**, 71, 2003.
32. Wei, M., Bullions, T. A., Rusa, C. C., Wang, X., Tonelli, A. E., *J. Polym. Sci. Part B, Polym. Phys. Ed*., **42**, 386, 2003.
33. Rusa, C. C., Uyar, T., Rusa, M., Hunt, M. A., Wang, X., Tonelli, A. E., *J. Polym. Sci. Part B, Polym. Phys. Ed*., **42**, 4182, 2004.
34. Wei, M., Shin, I. D., Urban, B., Tonelli, A. E., *J. Polym. Sci. Part B, Polym. Phys. Ed*., **42**, 1369, 2004.
35. Rusa, C. C., Shuai, X., Bullions, T. A., Wei, M., Porbeni, F. E., Lu, J., Huang, L., Fox, J., Tonelli, A. E., *J. Polym. Environ*., **12**(3), 157, 2004.
36. Pang, K., Schmidt, B., Kotek, R., Tonelli, A. E., *J. Appl. Polym., Sci*., **102**(6), 6049–6053, 2005.
37. Uyar, T., Rusa, M., Tonelli, A. E., *Macromol. Chem. Rapid Commun*., **25**, 1382, 2004.
38. Rusa, C. C., Wei, M., Bullions, T. A., Rusa, M., Gomez, M. A., Porbeni, F. E., Wang, X., Shin, I. D., Balik, C. M., White, J. L., Tonelli, A. E., *Crystal Growth Design*, **4**, 1431, 2004.
39. Rusa, C. C., Wei, M., Shuai, X., Bullions, T. A., Wang, X., Rusa, M., Uyar, T., Tonelli, A. E., *J. Polym. Sci. Part B, Polym. Phys. Ed*., **42**, 4207, 2004.
40. Rusa, M., Wang, X., Tonelli, A. E., *Macromolecules*, **37**, 6898, 2004.
41. Rusa, C. C., Wei, M., Bullions, T. A., Shuai, X., Uyar, T. A., Tonelli, A. E., *Polym. Adv. Technol*., **16**, 269, 2005.
42. Rusa, C. C., Rusa, M., Gomez, M. A., Shin, I. D., Fox, J. D., Tonelli, A. E., *Macromolecules*, **37**, 7992, 2004.
43. Hernandez, R., Rusa, M., Rusa, C. C., Lopez, D., Mijanos, C., Tonelli, A. E., *Macromolecules*, **37**, 9620, 2004.
44. Peet, J., Rusa, C. C., Hunt, M., Tonelli, A. E., Balik, C. M., *Macromolecules*, **38**, 537, 2005.
45. Harada, A., Okada, M., Kawaguchi, Y., *Chem. Letts*., **34**, 542, 2005.

46. Uyar, T., Rusa, C. C., Wang, X., Rusa, M., Hacaloglu, J., Tonelli, A. E., *J. Polym. Sci. Part B, Polym. Phys. Ed.*, **43**, 2578, 2005.
47. Rusa, C. C., Bridges, C., Ha, S.-W., Tonelli, A. E., *Macromolecues*, **38**, 5640, 2005.
48. Uyar, T., Rusa, C. C., Hunt, M. A., Aslan, E., Hacaloglu, J., Tonelli, A. E., *Polymer*, **46**, 4762, 2005.
49. Porbeni, F. E., Shin, I. D., Shuai, X., Wang, X., White, J. L., Jia, X., Tonelli, A. E., *J. Polym. Sci. Part B, Polym. Phys. Ed.*, **43**, 2086, 2005.
50. Uyar, T., Aslan, E., Tonelli, A. E., Hacaloglu, J., *Polym. Degrad. Stabil.*, **9**(1), 1–11, 2006.
51. Uyar, T., El-Shafei, A., Hacaloglu, J., Tonelli, A. E., *J. Inclus. Phenom. Macrocyclic Chem.*, **55**, 109, 2006.
52. Uyar, T., Hunt, M. A., Gracz, H. S., Tonelli, A. E., *Cryst. Growth Design*, **6**, 113, 2006.
53. Harada, A., Kamachi, M., *Macromolecules*, **23**, 2821, 1990.
54. Harada, A., Li, J., Kamachi, M., *Nature*, **356**, 325, 1992.
55. Harada, A., Li, J., Kamachi, M., *Nature*, **364**, 516, 1993.
56. Harada, A., Li, J., Kamachi, M., *J. Am. Chem. Soc.*, **116**, 3192, 1994.
57. Harada, A., Li, J., Kamachi, M., *Macromolecules*, **28**, 8406, 1995.
58. Harada, A., Suzuki, S., Okada, M., Kamachi, M., *Macromolecules*, **29**, 5611, 1996.
59. Harada, A. *Adv. Polym. Sci.*, **133**, 141, 1997.
60. Harada, A., Kawaguchi, Y., Nishiyama, T., Kamachi, M., *Macromol. Rapid Commun.*, **30**, 7115, 1997.
61. Harada, A., Nishiyama, T., Kawaguchi, Y., Okada, M., Kamachi, M., *Macromolecules*, **30**, 7115, 1997.
62. Kawaguchi, Y., Nishiyama, T., Okada, M., Kamachi, M., Harada, A., *Macromolecules*, **33**, 4472, 2000.
63. Harada, A., *Acc. Chem. Res.*, **34**, 456, 2001.
64. Huh, K. M., Ooya, T., Sasaki, S., Yui, N., *Macromolecules*, **34**, 2402, 2001.
65. Li, J., Ni, X., Leong, K., *Angew. Chem. Int. Ed.*, **42**, 69, 2003.
66. Choi, H. S., Ooya, T., Sasaki, S., Kwon, I. C., Jeong, S. Y., Yui, N., *Macromolecules*, **36**, 9313, 2003.
67. Li, J., Ni, P., Zhou, Z., Leong, K. W., *J. Am. Chem. Soc.*, **125**, 1788, 2003.
68. Choi, H. S., Takahashi, A., Ooya, T., Yui, N., *Macromolecules*, **37**, 10036, 2004.
69. Shin, K., Dong, T., He, Y., Taguchi, Y., Oishi, A., Nishida, H., Inoue, Y., *Macromol. Biosci.*, **4**, 1075, 2004.
70. Dong, T., He, Y., Shim, K., Inoue, Y., *Macromol. Biosci.*, **4**, 1084, 2004.
71. Dong, T., He, Y., Zhu, B., Shin, K., Inoue, Y., *Macromolecules*, **38**, 7736, 2005.
72. Nepal, D., Samal, S., Geckeler, K. E., *Macromolecules*, **36**, 3800, 2003.
73. Girardeau, T. E., Zhao, T., Leisen, J., Beckham, H. W., Bucknall, D. G., *Macromolecules*, **38**, 2261, 2005.
74. Rusa, C. C., Rusa, M., Peet, J., Uyar, T., Fox, J., Hunt, M. A., Wang, X., Balik, C. M., Tonelli, A. E., *J. Inclus. Phenom. Macrocyclic Chem.*, **55**, 185, 2005.
75. Liu, L., Guo, Q-X., *J. Inclus. Phenom. Macrocyclic Chem.*, **42**, 1, 2002.
76. Tonelli, A. E., *Macromolecules*, **24**, 1275, 1991.
77. Tonelli, A. E., *Macromolecules*, **25**, 3581, 1992.
78. Hunt, M. A., Rusa, C. C., Tonelli, A. E., Balik, C. M., *Carbohydr. Res.*, **339**, 2805, 2004.
79. Tonelli, A. E., *Computat. Theor. Polym. Sci.*, **2**, 80, 1992.
80. Vedula, J., Tonelli, A. E., *J. Polym. Sci. Part B, Polym. Phys. Ed.*, **45**, 735, 2007.

81. Hunt, M. A., Uyar, T., Shamsheer, R., Tonelli, A. E., *Polymer*, **45**, 1345, 2004.
82. Jia, X., Wang, X., Tonelli, A. E., White, J. L., *Macromolecules*, **38**, 2775, 2005.
83. Lu, J., Hill, M., Hood, M., Greeson, Jr., D. F., Horton, J. R., Orndorff, P. E., Herndon, S. A., Tonelli, A. E., *J. Appl. Polym. Sci*., **82**, 300, 2001.
84. Huang, L., Gerber, M., Lu, J., Tonelli, A. E., *Polym. Degrad. Stabil*., **7**(2), 279, 2001.
85. Romi, R., Lo Nostro, P., Bocci, E., Ridi, F., Baglioni, P., *Biotech. Prog*., **21**(6), 2005.
86. Busche, B. J., Rusa, M., Tonelli, A. E., Balik, C. M., *Macromolecules*, submitted.

# 13

# Polyolefin/clay nanocomposites

R. A. KALGAONKAR and J. P. JOG,
National Chemical Laboratory, India

## 13.1 Introduction

Composites are widely used in such diverse areas as transportation, construction, electronics and consumer products. They offer unusual combinations of stiffness, strength and weight that are difficult to attain separately from the individual components. The advent of nanoscience and nanotechnologies has continuously provided the impetus pushing for the development of materials with fascinating properties and a rich variety of applications. Polymer–clay (PC) nanocomposites represent a new class of materials based on reinforcement of polymeric materials by dispersion of nano-scale clay particles at molecular level in the polymer matrix. Because of their nanometer size features, nanocomposites possess unique properties typically not shared by their more conventional microcomposite counterparts and therefore offer new technology and business opportunities.

PC nanocomposites exhibit exceptional improvement in mechanical properties including stiffness, strength, dimensional stability as well as exhibiting barrier properties far better than conventionally filled polymers. In addition, because of the length scale involved that minimizes scattering, nanocomposites are usually transparent. Furthermore, PC nanocomposites exhibit a significant increase in thermal stability as well as self-extinguishing characteristics and enhanced flame retardancy.

Since PC nanocomposites achieve composite properties at much lower volume fraction of reinforcement, they avoid many of the costly and cumbersome fabrication techniques common to conventional fiber- or mineral-reinforced polymers. Instead they can be processed by techniques such as extrusion, injection molding and casting normally reserved for unfilled polymers. Furthermore, they are adaptable to films and fibers as well as monoliths. The combination of enhanced properties and weight reduction has already led to a few commercial applications. Toyota Motor Company has successfully introduced an automotive timing-belt cover made from nylon-layered silicate nanocomposite.[1] Ube Industries in Japan in collaboration

with Toyota is also developing nanocomposite barrier films for food packaging and other applications. Similar R&D efforts focusing on silicate nanocomposites are already underway in several US companies. Potential applications include airplane interiors, fuel tanks and components in electrical or electronic parts, under-the-hood structural parts, brakes and tires.

Polyolefins (POs) represent one of most widely used polymeric materials. However, fabrication of PO-based clay nanocomposites still remains a serious challenge for researchers. This is mainly due to the nonpolar nature of POs and the highly hydrophilic nature of clays. In the past efforts have been made to fabricate PO/clay nanocomposites using a variety of strategies. In this chapter we present a systematic review of the ongoing and past research concerning a variety PO/clay nanocomposites. The developments in this area with respect to the type of PO and clay, preparation technique of the nanocomposite, compatibilization and organic modification strategies used, and their effect on the various properties of these nanocomposites are reviewed critically.

### 13.1.1 Layered silicate clay minerals

Natural clays are most commonly formed either by the *in situ* alteration of volcanic ash or by the hydrothermal alteration of volcanic rocks. Bentonite is a rock that consists of commonly known smectite or montmorillonite group clays as its major component and auxiliary minerals such as kaolin, quartz, gypsum and iron ore. Sodium or calcium bentonite is not itself a mineral name: more correctly, it is smectite clay composed primarily of the mineral montmorillonite having sodium or calcium ions as its predominant cations. Smectite or montmorillonite group clays are further classified into two subgroups, trioctahedral and dioctahedral smectite clays. Montmorillonite, beidilite and nontronite are trioctahedral smectite clays whereas hectorite and saponite are dioctahedral smectite clays. Montmorillonite is a three-layer mineral, formed by stacking of several layers of tetrahedron and octahedron sheets, electrostatically held together by isomorphic interlayer cations. As the electrostatic attraction is low, exposure to polar fluids such as water will cause the formation of a monomolecular layer of water between the silicate layers. The basis behind bentonite swelling is that the several layers of water dipoles can form into weak 'stacked' tetrahedral structures, causing the silicate layers to separate – this is termed intercrystalline swelling. Purity and quality of bentonite will vary, as per the depositional environment and subsequent weathering processes and also differs by region and deposit.

The lattice structure of trioctahedral smectite clays comprises an octahedral alumina sheet, sandwiched between two tetrahedral silica sheets. The structural details of trioctahedral smectite clay are given in Fig. 13.1. A single crystal lattice of montmorillonite is negatively charged owing to the isomorphism

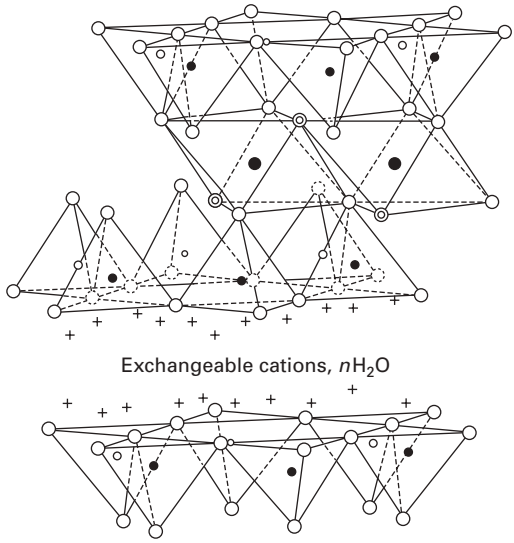


*13.1* Structure of smectite clay.

substitution mainly in the octahedral layer (e.g. $Mg^{2+}$ for $Al^{3+}$). The negative charge of the lattice is balanced by the exchangeable cations, which are held in the interlayer space of the clay. The exchangeable cations can be sodium and/or calcium ions, which can be replaced by suitable organic or inorganic cations.

The idealized unit cell formula of the sodium form of montmorillonite is $Na_{0.67}$ $[Al_{3.33}Mg_{0.67}]$ $[Si_8]$ $O_{20}$ $(OH)_4$ in which one of every six octahedral $Al^{3+}$ has been replaced by $Mg^{2+}$. The charge deficit is 0.67 electrostatic units (esu) per unit cell, or 0.67 equivalent charge per 734 g (formula weight) of clay. This gives a value of 91.3 milliequivalents (meq) charge deficit in a layer per 100 g of clay. This deficiency of charge must be balanced by equal quantity of cation charge at its surface for electrical neutrality. The maximum amount of any one cation that can be taken up by a particular clay is constant and is known as the cation exchange capacity (CEC) or base exchange capacity (BEC) of that clay. The amount is expressed in meq per 100 g of dry clay. CEC varies from 80 to 100 depending up on the substituted cation. Owing to the isomorphous substitution for $M^{3+}$ by $M^{2+}$ and $M^{2+}$ by $M^{+}$ in its structure, bentonite clay has a unique nature of cation exchange and adsorption capacity. The adsorption efficiency of bentonite is greatly enhanced after purification and/or modification. These properties have been used for a long time to decolorize edible oils, clarify alcoholic beverages and remove grease from raw wool.

## 13.2 Organomodification of clays

The smectite clay possesses a large surface area (~750 $m^2$/g). In order to utilize their high surface area efficiently, the chemical modification of such clays is necessary. During modification the exchangeable interlamellar cations are replaced by the other cations, inorganic or organic, present in the external environment. This can be achieved by several methods and the modified products obtained can be classified into various categories including acid-treated clays, pillared clays and nanoclays. Of particular interest in polymer/clay nanocomposites are nanoclays.

Nanoclays are complexes derived from clay–organic reactions. The clays used are smectite group clays, generally montmorillonite or hectorite. These clays are hydrophilic and accessible to intercalation. Therefore, they are liable to intercalate organics through ion exchange and/or adsorption when reacted with organic compounds and to be transformed to hydrophobic or organophilic nature. The organophilicity is ascribed to the interlamellar surface coverage with organics. Owing to the organophilic nature, the modified clays are named organophilic clays or organoclays.

Despite ignorance of the scientific basis of such interaction process, the uptake of certain organic compounds by clays has been known for a very long time, being the basis of a wide use of clays. Such clays are generally named 'bleaching' or 'Fuller's earth'. Complex-forming compounds may be classified into the following groups:

- uncharged polar organic compounds (neutral organic compounds);
- negatively charged organic compounds (acidic organic compounds); and
- positively charged organic compounds (basic organic compounds).

The nanoclays of particular interest with respect to usage of clay as a nanofiller in polymer composites are prepared by modification of clay using positively charged organic compounds. This class includes the organic compounds such as quaternary ammonium compounds (quaternaries), amines, alkaloids, purines, nucleosides, proteins, etc. The properties and end use of clays modified by such organic bases are largely dependent on the organic compound adsorbed by the clays.

### 13.2.1 Structure and properties of organomodified clays

The organomodified clays are prepared by reacting more voluminous organic onium cations with the montmorillonite clay. The reaction results in the exchange of relatively small sodium ions with organic counter-ions. This ion exchange results in the increase of the clay interlayer space, enabling organic cation chains to move in between the layers. In addition, the surface properties of each clay sheet are changed from being hydrophilic to hydrophobic.

During the cation exchange reaction the organic cations could either replace the inorganic cations or neutralize the hydrogen ions at clay surfaces.[2–4] Hendricks[5] concluded from his work that the adsorption of organic cations by clays is influenced both by electrostatic (columbic) and van der Waals attractive forces. Grim *et al.*[6] found that in the case of organic cations of relatively small size the maximum amount adsorbed did not go beyond the CEC of the clays, even when a large excess of the organic ion was present in the solution. Under similar conditions larger organic ions were taken up in the excess of the CEC because of the influence of van der Waals forces on the adsorption of large organic cations by clays. Similar findings were reported by Cowan and White[7] using isotherms for the adsorption of a homologous series of primary *n*-alkyl ammonium ions from ethyl ($C_2$) to tetradecylammonium ($C_{14}$) by sodium montmorillonite. Vansant and Uytterhoeven[8] concluded that apart from van der Waals forces of organic cations, the combination of variation in hydration status of the cations and electrostatic interactions between cation and clay surface played an important role in adsorption of *n*-alkyl ammonium ions on Na-montmorillonite.

On interaction with clay particles, the cationic portion of positively charged organic salts are accommodated in the interlayer space of clay crystals by replacing inorganic cations initially present. The interaction between the clay platelets and organic cations results in the replacement of $Na^+$ cations by organic cation moieties, which leads to an increase in the basal spacing. Barrer and Brummer found this increment to be directly related to the amount of organic cations present after the ion exchange.[9] Uncharged organics having strongly polar groups adopted an alpha-II orientation.[10] Jordan[11] observed a similar orientation in montmorillonite complexes with primary *n*-alkyl ammonium ions of varying chain length (from $C_3$ to $C_{18}$). He further concluded that the basal spacing values were sensibly constant at 1.36 nm for $C_3$ to $C_{10}$ and 1.76 nm for $C_{10}$ onwards. Further, when the cation area was smaller than half the area per exchange site, the amine cation adsorbed on one surface was found to be fitted into the gaps between the cations lying on the opposing surface to form monolayer complexes. When the area of the cation was greater than half the area per exchange position, interpenetration of this kind could not be realized and double layer complexes formed (e.g. for *n*-hexadecyl ammonium). Jordan *et al.*[12], using X-ray diffraction (XRD), observed the following results for a long chain cation such as *n*-octadecyl ammonium: (a) the formation of double layer complexes when the amounts of cations adsorbed were equivalent to the exchange capacity, (b) the alkyl chain in the double-layer complex stands at an angle to the silicate layer at amounts adsorbed higher than the CEC, and (c) at still higher amounts adsorbed, the chains were found reoriented into near-vertical positions with respect to the surface giving rise to a close packed arrangement which allows extensive van der Waals interactions between adjacent alkyl chains to be established. Greene-

Kelly[13] reported similarly for pyridinium and its derivatives in montmorillonite. Thus, besides being dependent on the alkyl chain length of the cation and the charge on the mineral layer, the arrangement of intercalated *n*-alkyl ammonium/pyridinium ions and/or molecules is also influenced by the amount of the cations and/or molecules adsorbed which ultimately depends on the amount of the compound reacted. The orientation of alkyl ammonium ions between the clay aggregates has been investigated by Lagaly.[14] He has reported that besides the formation of paraffin-type structures of chains in all-*trans* conformation, aggregates of chains containing *gauche* conformations are commonly observed. More recently, molecular dynamics simulations have provided insights into the packing orientation of alkyl ammonium surfactant chains in the clay interlayers.[15] It was observed that a disordered liquid-like arrangement of the *alkyl* chains was preferred in the clay gallery. In this disordered state the *alkyl* chains do not remain flat, but instead overlap and co-mingle with the adjacent onium ions in the opposing layers within the galleries.

## 13.3 Polymer/clay nanocomposites

PC nanocomposites are an emerging class of organic–inorganic hybrids that contain a relatively low wt% of nanometer-sized clay. These were first developed in the late 1980s. The dispersion of the nanometer-sized clay in the polymer matrix significantly improves the mechanical, thermal, barrier properties and flame retardancy of the base polymer. Three main types of nanocomposites can be obtained when clay is dispersed in a polymer matrix. This depends on the nature of the components used, including polymer matrix, clay and organic cation. If the polymer cannot intercalate between the silicate sheets, a microcomposite is obtained. The phase-separated composite that is obtained has the same properties as traditional microcomposites.

Beyond this traditional class of polymer–filler composites, two types of nanocomposites can be obtained. *Intercalated structures* are formed when a single (or sometimes more) extended polymer chain is intercalated (sandwiched) between the silicate layers. The result is a well-ordered multilayer structure of alternating polymeric and inorganic layers. *Exfoliated* or *delaminated structures* are obtained when the silicates are completely and uniformly dispersed in the continuous polymer matrix. The delamination configuration is of particular interest because it maximizes the polymer–clay interactions, making the entire surface of the layers available for the polymer. This should lead to the most significant changes in mechanical and physical properties. A schematic of the types of possible structure formations in PC composites is depicted in Fig. 13.2.

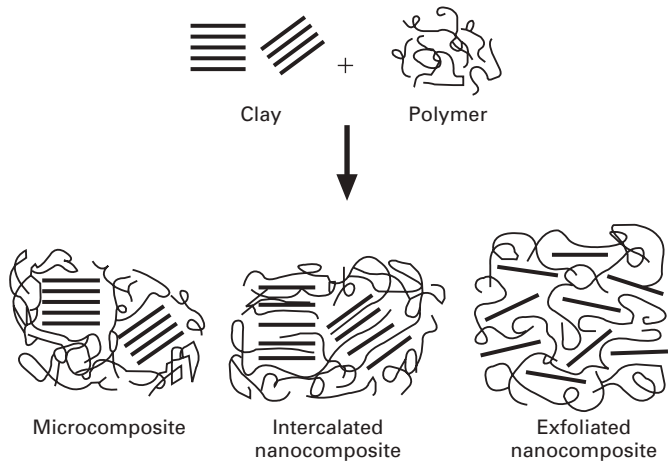


*13.2* Schematic representation of possible structure formation in PC composites.

### 13.3.1 Preparation techniques for polyolefin/clay nanocomposites

Different paths have been proposed to prepare PC nanocomposites, such as solution intercalation, *in situ* polymerization and melt intercalation.

*Solution intercalation*

This is one of the most common routes for preparation of PC nanocomposites. In this technique polar solvents are used to swell the organoclay followed by dissolving the polymer in the same solvent and mixing the two so that the polymer chains intercalate between the clay layers. The compensation of the decrease in the conformational entropy of the intercalated polymer chains by the entropy gained due to desorption of the solvent molecules is the driving force for polymer intercalation to take place using the solution intercalation technique. Although this is an advantageous method on the laboratory scale it is difficult to apply the solution intercalation method in industry owing to the problems associated with the use of large quantities of solvent.

*In situ polymerization*

This is a conventional process of synthesizing PC nanocomposites, especially those based on thermoset polymers. The organoclay is first swollen in the monomer. This requires a certain amount of time, which is governed by the polarity of the monomer molecules, surfactant molecules in the organoclay,

and the swelling temperature.[16] This is followed by the initiation of the reaction. The driving force for this mechanism is linked to the polarity of the monomer molecules: e.g., during the swelling phase, the high surface polarity of the clay attracts the polar monomer molecules so that they diffuse between the silicate layers. After reaching a certain equilibrium the diffusion stops and the layered silicate is swollen in the monomer to the extent equivalent to the perpendicular orientation of the alkyl ammonium surfactant.[17] When the polymerization is initiated, either by heat or radiation, by diffusion of a suitable initiator or by a catalyst fixed through cation exchange prior to the swelling step, the overall polarity of the intercalated molecules is lowered. This displaces the thermodynamic equilibrium so that more polar molecules are driven between the clay layers. This continuum eventually results in the organic molecules separating the clay layers.[18]

### *Melt intercalation*

Melt intercalation consists of blending a molten thermoplastic with an organically modified clay in order to optimize the polymer–clay interactions. It is a promising approach for forming nanocomposites that would greatly expand the commercial opportunities of this technology. The polymer chains have a significant loss of conformational entropy during the intercalation. The proposed driving force for this mechanism is the important enthalpic contribution of the polymer/organically modified clay interactions during the blending and annealing steps.

In the melt intercalation process, rheological and thermodynamic characters of the materials are important parameters that affect the degree of intercalation and properties of the final nanocomposites. Generally the degree of intercalation of the polymer in the organically modified clay is governed by matrix viscosity, average shear rate and mean residence time in the mixing process.

If technically possible, melt compounding could be significantly more economical and simple than *in situ* polymerization processes. This approach would allow nanocomposites to be formulated directly using conventional extruders and mixers as needed without the necessary involvement of resin producers. Indeed, PC nanocomposites have been successfully produced by extrusion. A wide range of thermoplastics, including strongly polar polyamide-6, ethylene vinyl acetate and polystyrene, has been intercalated between clay layers. However POs, which represent the biggest volume of polymers produced, have so far only been successfully intercalated to a very limited extent. As there are very few studies on formation of nanocomposites by direct melt intercalation, the corresponding knowledge of this process and its accomplishments is still far from complete.

### 13.3.2 Compatibilization issues in polyolefin/clay nanocomposites

Mere organophilization of the clay is often not sufficient to obtain intercalated or exfoliated PC nanocomposites. This is mostly true in the case of PO. This is mainly due to the low polarity of these polymers, which makes it difficult to get the exfoliation and homogeneous dispersion of the silicate layers at the nanometer level in the polymer. Silicate layers have polar hydroxyl groups, which are compatible only with polymers containing polar functional groups. This necessitates the use of a compatibilizer to facilitate the formation of an intercalated or exfoliated polymer/clay nanocomposite.

Another problem in the development of nanocomposites based on POs is the hydrophilic nature of the clay surfaces and the hydrophobic nature of PO. Thus the clay needs to be modified using suitable organic surfactants. The organically modified clay is adequate for most of the polar polymers, while for nonpolar PO, use of a compatibilizer is often required additionally to facilitate the intercalation of the polymer. The structure and properties of PC nanocomposites are governed by the choice of compatibilizer, its content and the nature of organic modifiers. A lot of work has been reported in polypropylene (PP)/clay nanocomposites using maleic anhydride (MA)-grafted PP as the compatibilizing agent.[19–33] The effectiveness of the compatibilizer depends on the molecular weight and the MA content. Higher MA content may facilitate melt intercalation; however, it may lead to immiscibility between the PP matrix and the compatibilizer. Most of the literature reports that the use of oligomers enhances the melt intercalation process, thereby resulting in better improvement in the mechanical properties. Generally the ratio of MA PP to clay used varies from 1:1 to 3:1. However, higher content of MA PP may not be cost effective and may also lead to inferior mechanical properties. In spite of lots of studies this truly exfoliated PP/clay hybrid cannot be prepared by melt mixing techniques.

Ding *et al.*[34] prepared PP/clay nanocomposites using a highly effective PP solid-phase graft as a compatibilizer (solid-phase graft contained MA and butyl acrylate as grafting monomers and had a grafting percentage of 11.8%). This technique facilitated increase in mechanical properties, thermal stability and crystallization temperature of the nanocomposites. Wang *et al.*[32] studied melt processed PP/clay nanocomposites modified with maleated PP compatibilizers. The organoclay was first blended with PP-g-MA. They used different grades of PP-g-MA with a wide range of MA content and molecular weight. PP/organically modified clay nanocomposites were then modified with different levels of PP-g-MA compatibilizers on a twin-screw extruder. They reported that although PP-g-MA with lower molecular weight and higher MA content could lead to good clay dispersion in PP/clay composites, it caused deterioration in both the mechanical and thermal properties of the

composites. They concluded that there were two important factors contributing to exfoliation and homogeneous dispersion of the clay layers: (1) intercalation capability of the compatibilizers in the clay layers and (2) the composition of the compatibilizer in PP/clay composite. Garcia-Lopez *et al*.[33] have studied the effect of compatibilizing agents on clay dispersion in PP/clay nanocomposites. For this purpose they prepared PP/clay nanocomposites using two different coupling agents, diethyl maleate (DEM) and MA, and two different clays. They observed that the differences in mechanical properties when using different clays are smaller if DEM is used instead of MA. They concluded that clay dispersion and interfacial adhesion are greatly affected by the kind of matrix modification.

## 13.4 Polypropylene/clay nanocomposites

PP is one of the most widely used PO polymers and a very attractive candidate for the matrix phase of polymer nanocomposites. However, as PP does not include any polar groups in its backbone, it was thought that the homogeneous dispersion of silicate layers in PP would not be possible. Earlier experimental approaches to intercalate PP in to the silicate layers involved using clays modified with nonpolar organic molecules.[35] In this approach a PO oligomer with telechelic OH groups, which was used as a compatibilizer, was first intercalated in the organically modified silicate layers through strong hydrogen bonding. This results in weakening of interlayer interaction through expansion of the silicate layers. A PP/clay hybrid was obtained by mixing PP with the organoclay modified using the functional oligomer. Although improved dispersion of the clay layers in PP was obtained through this process, some aggregates of the clay minerals were still observed in the hybrid. In a subsequent paper, Kawasumi *et al*. reported the use of MA-modified PP oligomers as compatibilizers.[20] They postulated that there are two important factors, that govern the homogeneous dispersion of clay layers and formation of the exfoliated PP/clay hybrid, viz. (1) the intercalation capability of the oligomers in the clay interlayers and (2) the miscibility of the oligomers with PP. In a following paper Hasegawa *et al*. reported the preparation of PP/clay nanocomposites using PP modified with MA by the melt intercalation technique.[36] On comparison of the dispersibility of the clay in the hybrid containing PP-g-MA with that containing homo-PP it was observed that the former did not show the presence of clay stacks while an apparent peak corresponding to the $d_{001}$ plane reflection of the clays was observed in the latter. Further, the homo-PP/clay hybrid showed the same *d*-spacing as that of the organoclay used in this study. This research served as the basis for the use of MA-grafted PP as the compatibilizer, which was widely applied as the compatibilizing agent in the fabrication of PP/clay nanocomposites over the following years.

Few approaches other than the usage of MA-g-PP have been reported for the preparation of PP/clay nanocomposites. Thermodynamically it is not possible to produce miscible nanocomposites of PP and alkyl ammonium modified clays without the assistance of solvents or extensive shear.[37] Along the same lines, Manias *et al*. developed two approaches. In the first approach, nanocomposites were formed by attaching minute amounts of polar functional groups to PP.[38] These functionalized PP derivatives were either attached to PP in blocks or randomly grafted so that the polymers still resembled the neat PP closely (only 0.5% functional groups) but at the same time had adequate polar character to become miscible with alkyl ammonium modified clays ether by direct melt intercalation or co-extrusion of PP with the organically modified PP. In the second approach, the formation of PP/clay nanocomposites was realized by using neat/unmodified PP and a semifluorinated surfactant modification for the clay. Here also nanocomposite formation was achieved by direct melt interaction unassisted by shearing or solvents suggesting sufficiently favorable thermodynamic interactions between the PP and the clay. In both the cases microstructural characterization of PP/clay nanocomposites revealed a coexistence of intercalated and exfoliated clay layers throughout the polymer matrix. These nanocomposites exhibited enhanced mechanical properties, including higher moduli and strength, and at the same time were found to be thermally more stable than neat PP as well as exhibiting enhanced flammability characteristics. Moreover they were found to be more resistant to solvents and to have improved starch resistance compared with neat PP.

In a subsequent paper, Manias and coworkers proposed another novel approach for the preparation of PP/clay nanocomposites.[39] They used ammonium terminated PP as the organic modification for montmorillonite to obtain exfoliated PP/clay nanocomposites. They also show the advantage of chain-end-functionalized PP over side-chain-functionalized or block copolymer PP to obtain exfoliated structures rather than intercalated ones. Sun and Garces reported a novel synthesis approach to make high-performance PP/clay nanocomposites by *in situ* polymerization with metallocene/clay catalysts under mild polymerization conditions, which resulted in great improvements in mechanical performance and processability of the polymer.[40] This approach is free from the usage of any external activators needed for initiating the olefin polymerization and also high pressure and temperature process conditions are not required.

Kato *et al*. have reported a new production method for PP/clay nanocomposites.[41] The highlight of this method was a lack of prior organic modification of clay. This method focuses on the nature of the clay mineral, which was exfoliated in water. By controlling the pressure of the water vapor, the exfoliation of the clay mineral was achieved in a twin-screw extruder. Two compatibilizers, MA-modified PP and octadecyl trimethyl

ammonium chloride, were added to the mixture of the clay mineral and PP to prevent aggregation of the clay in the twin-screw extruder. The PP/clay nanocomposite thus formed consisted of exfoliated clay layers, which were dispersed uniformly in the polymer matrix as evidenced by XRD and transmission electron microscopy (TEM) studies. The PP/clay nanocomposite had almost the same excellent properties as a conventional PP/clay nanocomposite. The obvious advantage of this method is the elimination of the organic modification of the clay, which has to be carried out separately from the melt compounding in an extruder. The process of organic modification of clay, which consists of various industrial processes of agitation, filtration, drying and milling, can be cumbersome and is also costly. Thus, the elimination of organic modification will simplify the overall process of PC nanocomposite production as well as reduce the cost of the final product as compared with PC nanocomposites prepared using the conventional processes. However, the successful implementation of this process for other polymers is yet to be demonstrated.

For the successful production and application development of PP/clay nanocomposites a better understanding of the structure–property relationships in these multicomponent systems from the point of view of a wide spectrum of variations in the nature of ingredients and processing environments is necessary. Taking this into consideration one of the major criteria governing the performance of PP/clay nanocomposites is the inherent structure of the organically modified clay. The specific variations imposed on the organically modified clays involve the initial interlayer spacing and the packing density of the organic chains within the clay gallery space.[30, 42] During the process of intercalation, the polymer chains penetrating the clay layers have to overcome a large entropy barrier, which is a result of the closely packed clay layers. The entropy barrier can be lowered by favorable enthalpic contributions that are possible by modification of the clay using suitable organic moiety such that the polymer–clay interactions are more favorable than the clay–surfactant interactions. Increasing the modifier concentration of the surfactant leads to a more efficient packing and increased interlayer contact between the clay layers, resulting in more cohesive van der Waals interactions between the clay layers and, thus, a greater interlayer solid-like character. Formation of intercalated hybrid will be favored in systems with favorable enthalpic contributions, which are possible when polymer–clay interactions are more favorable than the clay–intercalant interactions. Thus, systems that contain organically modified clays with intercalant concentration, which is thermodynamically favorable to compensate for the loss of conformational entropy by enthalpic gains when the clay comes in contact with polymer chains, are more likely to have a higher amount of polymer intercalated in the clay interlayer. Hence, higher intercalant concentration in the clay interlayer makes it more dense and reduces the polymer–clay interactions, which in

turn makes it harder for the free polymer chains to infiltrate the clay gallery space.

To understand the mechanisms underlining the property enhancements observed in PC nanocomposites it is necessary to understand how the nanomorphologies of these advanced materials influence their properties. Gilman *et al.* have studied the flammability properties of PP/clay nanocomposites to understand the use of these nanocomposites as flame retardants.[43] The type of clay, level of dispersion in polymer matrix and processing degradation influence the magnitude of the flammability reduction in PP/clay nanocomposites. It is concluded that a high-performance carbonaceous-silicate char builds up on the surface during burning, which insulates the underlying material and slows down the mass loss rate of decomposition products. Zanetti and coworkers reported the flame-retardant properties based on PP–graft–MA and organically modified clays using oxygen consumption cone calorimetry.[44] The effect of addition of traditional flame retardants, viz. decabromodiphenyl oxide (DB) and antimony trioxide (AO), to the nanocomposites was investigated by cone calorimetry and conventional flame-retardant evaluation techniques such as limiting oxygen index and vertical burning test. For comparison, the flammability properties of the PP/clay nanocomposites were studied both in the presence and absence of DB and AO. The nanocomposites showed better flame-retardant properties than the pure polymer. The peak heat release rate reduced still further with the use of AO or BD. When both the additives were added to the nanocomposite a synergistic effect results, which did not occur under identical testing conditions, when AO and BD were added to the pure polymer.

Thermal characteristics of PP/clay nanocomposites and the organically modified clays used as nano fillers were investigated by Lee *et al.* using XRD, TEM and Fourier transform infrared (FTIR) spectroscopy as characterization tools.[45] Two organically modified clays containing different alkylammonium surfactants were used in this study. The PP/clay nanocomposites were prepared by melt blending of the polymer with the organically modified clays and MA-grafted PP oligomer as a compatibilizer. The modified clays showed decrease in the interlayer spacing at the processing temperature due to thermal decomposition of the organic cation. It was observed that the thermal characteristics of the modified clays are dependent not only on the type of alkylammonium surfactant but also on the interlayer structure. Partial exfoliation of PP composite was observed during processing at high temperatures, using the alkylammonium-modified clay containing ethoxy groups (A), which initially had a small interlayer spacing and polar character. This behavior was attributed to the decrease in the interlayer spacing and less surface organophilicity due to thermal decomposition of this clay during processing. The PP/clay nanocomposite prepared using the modified clay containing the alkylammonium surfactant with purely aliphatic chains (B)

exhibited the formation of intercalated or exfoliated structure. This difference in behavior was because the clay B was more organophilic initially compared with clay A, which led to melt intercalation in spite of thermal decomposition, resulting in intensive intercalation or exfoliation aided by shear.

Crystallization can be used effectively to control the amount of polymer intercalating the clay gallery space, which in turn will control the morphology, mechanical and other properties of PC nanocomposites. Jog and coworkers were first to report the crystallization behavior and the morphology of PP/clay nanocomposites prepared by melt processing and using PP–graft–MA as the compatibilizer.[27, 28] They found that the PP/clay nanocomposites crystallize at a higher temperature than pure PP. Also the spherulitic morphology of PP is completely altered in PP/clay nanocomposites, which crystallize in the form of peculiar birefringent structures, which grow with time. This indicates that the surface of the exfoliated clay layers acts as a nucleating agent that promotes crystallization in PP. Isothermal crystallization studies on PP/clay nanocomposites revealed that the nanocomposites exhibit a narrower isothermal crystallization peak than pure PP. The PP/clay nanocomposites exhibited lower values of total crystallization time, indicating that the crystallization process of PP is accelerated in the presence of clay. In a subsequent paper Jog and coworkers reported similar observations from the isothermal crystallization studies carried out on PP/clay nanocomposites prepared using three different grades of PP, two grades of MA-grafted PP containing different percentages of MA and two clays.[29] Okamoto and coworkers reported the crystallization behavior of three different PP/clay nanocomposites.[46] They found that the linear growth rate of the spherulites and the overall rate of crystallization is not influenced by the presence of clay. XRD studies revealed that the intergallery spacing increases with increasing crystallization temperature ($T_c$) and at constant $T_c$ the extent of intercalation increased with decreasing clay content. TEM observations revealed that clay particles are well dispersed at low $T_c$, while segregation of clay layers occurs at high $T_c$. Dynamic mechanical analysis (DMA) shows that the storage modulus ($G'$) increases with increasing $T_c$. This increase is limited to 30% for nanocomposites with low clay content (4 wt% clay) and it decreases to lower values with increasing clay content. Thus, by controlling the intercalation through crystallization at a suitable temperature the microstructure, morphology and mechanical properties of crystalline PC nanocomposites can be controlled.

DMA is an important tool for studying the structure–property relationships in polymer composites. DMA essentially probes the relaxations in polymers, thereby providing a method to understand the mechanical behavior and the molecular structure of these materials under various conditions of stress and temperature. Hasegawa *et al*. reported the mechanical properties of PP/clay nanocomposites prepared using MA-modified PP oligomer as a com-

patibilizer.[22] The storage moduli values observed for PP/clay nanocomposites were found to be higher than those of pure PP up to 130 °C. The relative storage moduli of PP/clay nanocomposite to those of pure PP were studied to understand the effect of clay hybridization. These values were found to be relatively small below the glass transition temperature ($T_g$) of PP; however, above $T_g$ they drastically increased and then decreased to melt. This tendency was emphasized more strongly as clay layers were more uniformly dispersed in the PP matrix. The relative storage moduli of poorly dispersed clay layers were found to be relatively small and almost independent of temperature. Jog and coworkers have reported that the PP/clay nanocomposites exhibit higher storage moduli (increase of about 56%) than neat PP over the entire temperature range studied (–40 to 120 °C).[27, 28] The loss modulus that corresponds to the dissipation of the energy shows a peak at about 11 °C for PP, which corresponds to the glass transition temperature of PP. In PP/clay nanocomposites, this peak is not well defined. It was thus concluded that the cooperative relaxation of PP in the nanocomposites becomes weak owing to the restricted mobility of the chains in the presence of the clay layers.

There are many reports in the literature that show remarkable improvements in the tensile properties of the polymeric materials when organically modified clays are used as nano-fillers. A combination of improved stiffness and strength is only possible when either intercalated or exfoliated nanocomposites having uniformly dispersed clay platelets are formed. Better stress transfer between the filler and the polymer will result in improved mechanical properties of the polymer composite. This is possible with the formation of nanostructures. Reichert *et al*. have systematically evaluated the influence of organic modification of clays and compatibilizer functionality on the structure and properties of PP/clay nanocomposites using a series of organophilic clays modified using various protonated alkyl amines and two types of PP–graft–MA oligomers with different anhydride functionalities.[24] The results showed that tensile property enhancement was possible only when a specific compatibilizer was used in combination with appropriate organically modified clays. Jog *et al*. reported an enhancement in the flexural properties of PP/clay nanocomposites prepared by melt blending.[27] The flexural modulus increased by 30% while the flexural strength increased by 25% compared with neat PP. An increase in the tensile modulus and tensile strength of the nanocomposites was also reported. The improved mechanical properties depended on the type of organic modifier and the inorganic content of the clay. It was observed that the clay containing more inorganic matter showed better improvement than that containing less.

A rheological study of polymer nanocomposites is of great importance considering their fabrication and final applications. Rheology is a powerful tool, which provides important information on the internal microstructure of the nanocomposites, the state of dispersion of the clay, its orientation and

aspect ratio, as well as the effects of particle–particle interactions in clay and particle–polymer interactions on the viscoelastic behavior of the nanocomposites. Therefore, an understanding of the viscoelastic properties of polymer nanocomposites, both in solid and molten state, is essential from a processability and structure–property point of view.

Dynamic oscillatory shear experiments are representative of the durability of the sample under various conditions of vibrations and/or external stress. Galgali *et al*. have studied the rheological response of isotactic PP/clay nanocomposites in the presence and absence of the compatibilizer, viz. PP–graft–MA.[47] They show that the nanocomposites show a solid-like rheological response at low frequencies, which is completely dependent on the amount of clay loading in the nanocomposites, and is independent of the finer structure of the nanocomposites, i.e. whether they are end-tethered or melt intercalated. They also show that the typical rheological response of the PC nanocomposites does not arise due to restricted mobility of the confined polymer chains between the clay galleries, but is an effect of the frictional interactions between the clay layers. Further they have shown that beyond the apparent yield stress the zero shear viscosity of the PP/clay nanocomposite containing 7 wt% clay and the compatibilizer drops dramatically by more than three orders of magnitude, suggesting that the solid-like behavior of the PP/clay nanocomposites after annealing is due to the formation of a percolating network that strongly resists deformation. Recently, Abranyi *et al*. reported through rheological investigation that a percolated clay network formation is possible only under certain conditions.[48] Accordingly, at low clay content a higher degree of exfoliation is needed to produce the number of silicate layers to form a percolated structure. When the clay content is higher, which increases the number of individual platelets, the amount of compatibilizer required for the formation of the network is less. To summarize a threshold concentration of MAPP exists in PP/clay nanocomposites for the formation of the clay network, which depends on the silicate content.

Lele *et al*. studied the rheology–microstructure links in syndiotactic PP/clay nanocomposites using *in situ* rheo-X-ray measurements of the nanocomposites during shear.[49] The microstructure of the nanocomposite at low strain and shear rates consisted of a percolating three-dimensional network of dispersed clay tactoids. Rheology indirectly indicated that the observed yielding of the material at high stresses might be linked to the orientation of the clay tactoids, which was evidenced using the rheo-X-ray diffraction measurements. The transient experiments showed that the clay tactoids relax their orientation incompletely after cessation of shear. It was observed that the stress relaxation of the matrix chains, which were compatibilized with clay platelets, drives the orientation relaxation in about $10^{-3}$ s. After this time scale the clay tactoids are jammed and produce a percolating network having a residual orientation and a residual relaxation modulus. In steady

shear experiments at shear rates below $10^{-3}$ $s^{-1}$ the response corresponding to that of a percolating network would be observed while at shear rates above $10^{-3}$ $s^{-1}$, a yield-like response would be observed.

Okamoto *et al*. investigated the elongational flow-induced structure formation of PP/clay nanocomposites by carrying out uniaxial elongational tests at constant Hencky strain in molten state using elongational flow optorheometry.[50] The PP/clay nanocomposites exhibited high viscosity and a tendency of strong strain-induced hardening. This was attributed to the perpendicular alignment of the clay layers to the stretching direction. They observed two features from the shear viscosity curve. First, the extended Trouton rule is invalid for PP/clay melt, in contrast to the melt of ordinary homopolymers. Second, the shear viscosity of the PP/clay melt increases continuously with time without reaching the steady state within the time spans studied. This time-dependent thickening behavior is termed as rheopexy. These differences reflect the difference in the shear flow-induced versus elongational flow-induced internal structure fomation in PP/clay nanocomposite melts. Rheopexy was not observed for PP homopolymer modified with PP–graft–MA melts.

TEM results were presented for the nanocomposites along the *x*- and *y*-axes of the elongated specimens, which represented the directions parallel and perpendicular to the stretching direction. A converging flow is applied to the thickness direction (*y*- and *z*-axis) with stretching if the assumption of affine deformation without volume change is valid. For the specimen elongated with high strain rate, perpendicular alignment of the clay layers (edges) was observed along the stretching direction (*x*-axis) in the *x*–*y* plane. For the *x*–*z* plane, the clay layers (edges) disperse into the PP matrix along the *z*-axis direction rather than randomly, but these faces cannot be observed in this plane. From the experimental results and the two-directional TEM results the authors conclude the formation of a house of cards-like structure under slow elongational flow.

## 13.5 Polyethylene/clay nanocomposites

Polyethylene can be used for a wide range of applications because, depending on its structure, it can be produced in many different forms. Low-density polyethylene (LDPE) was the first type of polyethylene to be commercially exploited. It can be characterized by a large degree of branching, forcing the molecules to be packed rather loosely, forming a low-density material. LDPE is soft and pliable and has a variety of applications including plastic bags, containers, textile and electrical insulation, as well as coatings for packaging materials. There have been few attempts to develop nanocomposites based on LDPE and clays for improvement in materials properties. Morawiec *et al*. reported the preparation of nanocomposites based on compatibilized LDPE

and organically modified clays.[51] The nanocomposites were prepared by melt-mixing MA-grafted LDPE with octadecyl amine-treated clay in an internal mixer. Improved thermal stability in the nanocomposites was observed which was attributed to the exfoliation of the clay platelets in the polymer matrix. Further, it was observed that the uncompatibilized LDPE/clay composite fractures early during drawing due to decohesion of the polymer from non-exfoliated clay platelets and did not exhibit improved thermal properties. The nanocomposite containing more compatibilizer could be deformed to a higher elongation. The authors argued that the mechanical performance of these nanocomposites is not only governed by clay exfoliation and clay content but also by the presence of a significant amount of compatibilizer, which is reflected in the above result. They concluded that MA-grafted polyethylene not only promotes the exfoliation of the clay and its good adhesion as compared with pristine LDPE but also toughens the polymer matrix.

In an earlier study Antipov *et al*. reported the structure and deformation behavior of LDPE/clay nanocomposites.[52] The effects on the type and concentration of a filler on the structure and deformation behavior of LDPE/clay nanocomposites was studied. The clay was organically modified using various substrates. From the crystallization study it was observed that a part of the polymer crystallizes on the surface of layered silicate particles as heterogeneous nuclei, giving rise to a finely crystallite fraction and a bimodal crystallite size distribution. The nanocomposites showed an improved Young's modulus, while the tensile strength and elongation at break decreased compared with the pristine polymer. They also argued that the cold drawing of composite films decreases the dimensions of the crystallites by more than two orders, although the melting temperature of LDPE in the nanocomposite with oriented clay platelets remained almost the same as in the isotropic pure polymer film.

### 13.5.1 Linear low-density polyethylene/clay nanocomposites

Earlier research on linear low-density polyethylene (LLDPE)/clay nanocomposites focused on the preparation of LLDPE-based clay nanocomposites via *in situ* ethene homo- and copolymerization as well as by the melt compounding technique.[53] It was observed that, compared with melt compounding, *in situ* polymerization, catalyzed with methylaluminoxane-activated zirconocene, nickel and palladium catalysts, was more effective in the formation of LLDPE/clay nanocomposites as evidenced by larger interlayer spacing and formation of exfoliated anisotropic nanoclays with high aspect ratio.

Another method for the preparation of LLDPE/clay nanocomposites was reported by Wang *et al*.[54] They used MA-grafted polyethylene to prepare the

nanocomposites via the melt compounding technique. It was observed that the morphology of the LLDPE/clay nanocomposite (intercalated or exfoliated structure) was governed by the hydrophobicity of the organically modified clay and the hydrophilicity of the maleated polyethylene. It was also observed that in case of hybrids prepared with neat LLDPE, the intercalation capability of the polymer depended upon the thermodynamical equilibrium state at the clay surface rather than the initial interlayer spacing of the organophilic clay.

Recently, Sanchez-Valdes *et al*. reported the preparation of LLDPE/clay nanocomposites using a zinc-neutralized carboxylate ionomer as a compatibilizer.[55] The results so obtained were compared with the nanocomposites prepared using LLDPE–graft–MA as compatibilizer. The nanocomposites prepared with ionomer showed good mechanical performance only slightly below that of the nanocomposites prepared using MA. This was attributed to the interactions between the ionomer functional groups and the polar groups in the clay surfactant and the nano-size of the clay, as well as the uniform dispersion of the clay in the polymer matrix. The oxygen permeability of the nanocomposites prepared using the ionomer was decreased by the addition of the clay. It was concluded that ionomeric compatibilization not only promotes the exfoliation of clay but also improves adhesion to LLDPE, and increases the mechanical performance of the polymer.

Lew *et al*. reported the preparation of LLDPE/clay nanocomposites from metallocene-catalyzed and conventional Ziegler–Natta-catalyzed LLDPE by melt compounding.[56] Owing to higher extrusion shear stress, attributed to a narrower molecular weight distribution, metallocene-catalyzed LLDPE was found to be more effective in exfoliating the clay layers than that synthesized from Ziegler–Natta catalyst. It was also shown that the polymer chain-branching, clay exfoliation, and PE–graft–MA compatibilizer concentration have significant effects on the three $\alpha$, $\beta$ and $\gamma$ relaxation temperatures. Further it was observed that the degree of crystallinity increased with the addition of the compatibilizer PE–graft–MA and the presence of clay platelets appeared to have suppressed the overall crystalline lamellar formation as a result of restricted chain mobility.

Hotta and Paul studied the effect of the use of organic modification (they have used clays modified with different alkyl ammonium modifiers, viz. having one alkyl tail and having two alkyl tails) on the morphology and mechanical properties of LLDPE/clay nanocomposites.[57] The effect of use of LLDPE–graft–MA as a compatibilizer was also investigated. Nanocomposites derived from organic clay modified with two alkyl tails exhibited better clay dispersion and improvement in the mechanical properties as compared with that derived from the organically modified clay having only one alkyl tail. This behavior was attributed to the better affinity of LLDPE for the alkyl tails; thus increasing their number resulted in better

dispersion of clay in the LLDPE matrix. The rheology and gas permeability of the nanocomposites derived from the organically modified clay having two alkyl tails were also investigated and the results showed that both melt viscosity and melt strength increased with increased clay content and LLDPE–graft–MA content, while the gas permeability decreased by the addition of the clay.

### 13.5.2 High-density polyethylene/clay nanocomposites

High-density polyethylene (HDPE) is a version of polyethylene that is defined by its higher density (greater than or equal to 0.941 g/cm$^3$). It is harder, stronger and a little heavier than LDPE, but less ductile. It has a low degree of branching, thus stronger intermolecular forces. HDPE has an opaque wax-like appearance and its properties include good flexibility, good low temperature toughness, good resistance to chemicals and weathering, good processability by most of the processing techniques, and it is less expensive. HDPE is known to have poor barrier properties for gases, solvents and hydrocarbons. Thus, enhancement of barrier, mechanical and thermal properties of HDPE through incorporation of clay and formation of nanocomposites can open new avenues of applications for HDPE.

Bafna *et al*. prepared HDPE/clay nanocomposites using a melt extrusion technique and maleated LDPE as a compatibilizer.[58] They reported a study on the three-dimensional (3D) hierarchical orientation of six different structural features of these nanocomposites using two-dimensional (2D) small-angle X-ray scattering and 2D wide-angle X-ray scattering. The structural features studied included: clay clusters/tactoids (120 nm), modified clay (002) (2.4–3.1 nm), unmodified clay (002) (1.3 nm), clay (110) and (020) planes normal to the previous two, polymer crystalline lamellae (001) (19.0–26.0 nm), and polymer unit cell (110) and (200) planes. The orientation data showed two surprising results. First, the clay tactoids are associated with the intercalated clay and not with the unmodified clay. Secondly, the unmodified clay is associated with the polymer lamellae and may modify the lamellar surface energy. By tuning the clay platelet orientation, the permeation and strength of the PO films could be controlled. They concluded that it is the lamellae and not the chains that govern the final orientation of the polymer crystals, since chain tilt leads to randomization of the unit cells and not the lamellar normals.

Osman and Atallah have reported a comparative study on the effect of filler particle shape, size and surface treatment on polymer crystallinity and gas permeability using spherical and plate-like inclusion in HDPE.[59] Plate-like inclusions strongly reduce the polymer permeability coefficient while the spherical particles do not have any effect on it. The reduction in gas permeability depends on the average aspect ratio of the fillers, which in turn

depends on the exfoliation of the clay and consequently on its surface tension. Neither the spherical particles (calcium carbonate modified and unmodified) nor the plate-like particles (organically modified clay) were found to nucleate crystallization of HDPE under slow cooling conditions. In a following paper Osman *et al*. reported the gas permeability properties of HDPE/clay nanocomposites of organically modified clays having different surface coverage and alkyl chain packing density.[60] An appreciable decrease in the permeation coefficient of the composites was observed for partially exfoliated clays in the polymer matrix.

Xu *et al*. reported that on grafting with acrylic acid, the dispersion and intercalation of bentonite clay in HDPE/clay nanocomposite increased.[61] Consequently, with increasing clay content in the nanocomposite formed with acrylic acid grafted HDPE, the tensile strength and Young's modulus increased, while that of neat HDPE/clay nanocomposites decreased. Also the addition of clay to the grafted polymer was found to affect the melting temperature and the degree of crystallization of the matrix; by decreasing these values, however, no change was observed in the crystallization behavior of the neat HDPE/clay composite.

Tanniru *et al*. studied the mechanical response of HDPE/clay nanocomposite. The micromechanism of plastic deformation during impact loading is studied with scanning electron microscopy (SEM), and the impact strength of the composites is linked to the structural studies performed using differential scanning calorimetry (DSC), DMA, and TEM and SEM.[62] With the addition of clay the impact strength of HDPE decreases; however, the toughness continued to be higher even at very low temperatures. It was observed that the fracture of HDPE initiates with crazing, while the propagation zone involves a combination of different processes, viz. fast propagation of crack and shear process. The fracture initiation and propagation of HDPE/clay nanocomposites is characterized by stretching of fibrils (fibrillation) interdispersed with microvoids. The low toughness of the nanocomposites in relation to neat HDPE is related to the crystal structure and the interfacial interaction between the filler and the polymer matrix. The primary mechanism of deformation in the nanocomposites is altered from a combination of craze and drawing of fibrils in HDPE to a microvoid coalescence-fibrillated process.

### 13.5.3 Ultra-high molecular weight polyethylene/clay nanocomposites

Ultra-high molecular weight polyethylene (UHMWPE) has extremely high abrasion resistance when compared with other thermoplastics. It also has exceptional impact resistance, even at cryogenic temperatures, and is superior to stainless steel. Other advantages of UHMWPE include: low moisture absorption, good electrical and thermal insulation, self-lubrication and chemical

inertness (except in some acids). Some formulations in which UHMWPE can be used are sheet, rod and tube. Some of its excellent uses are as wear strips, chain guides, chute and hopper linings, bushings, and boat and truck bed liners. Recently Park *et al*. reported the preparation and characterization of UHMWPE/clay nanocomposites by using the melt intercalation technique.[63] XRD analysis of the nanocomposites indicated that the nanocomposites were formed upon exfoliation of the clay layers in the polymer matrix. The thermal stability of the nanocomposites increased with increasing clay content compared with the pristine polymer as evidenced from the thermogravimetric analysis (TGA) results. This was attributed to the tortuous path encountered by the diffusing volatiles within the nanocomposites. The mechanical property studies of the nanocomposites showed that they exhibited higher tearing energies and tensile strengths than those of the pristine polymer. They concluded that the interfacial and mechanical properties of UHMWPE were improved upon addition of the clay and formation of the nanocomposite.

## 13.6 Higher polyolefin/clay nanocomposites

### 13.6.1 Poly(4-methyl-1-pentene)/clay nanocomposites

Poly(4-methyl-1-pentene) (PMP) is an important member of the PO family. It has wide-ranging application in various industries, including automotive components, light covers, as well as special medical applications such as pacemaker parts, blood collection and transfusion devices, medical and laboratory apparatus. It is also used for commodity applications such as microwave components, cookware and electronic components. Of particular interest are properties such as low density, higher thermal stability, chemical resistance, optical transparency and high permeability. However, there is a limitation on the applications of PMP as its mechanical properties deteriorate even at temperatures just above the ambient temperature. It is well known that incorporation of clay enhances the thermomechanical properties of the polymers. Thus, a study that focuses on this aspect through the formation of PMP/clay nanocomposites is of academic as well as industrial interest. However, very few studies have reported the preparation and properties of PMP/clay nanocomposites. Wanjale and Jog have fabricated PMP/clay nanocomposites using the melt intercalation technique.[64] They studied the effects of clay modification and compatibilizer on the formation and properties of the nanocomposites. Two commercially available organically modified clays were used for the preparation of PMP/clay nanocomposites. X-ray diffraction studies showed the formation of intercalated, disordered and/or partially exfoliated hybrids. The reinforcing effect of the clays was studied using DMA. The nanocomposite formed using the clay modified with dimethyl hydrogenated tallow 2-ethylhexyl-quaternary ammonium methyl-sulfate

showed better mechanical properties than that formed using the clay modified with dimethyl, dihydrogenated tallow quaternary-ammonium chloride. Although the addition of compatibilizer improved the *d*-spacing of the nanocomposites along with their thermal stability it failed to bring about much improvement in the storage moduli values in the rubbery regime. This was attributed to the low melting point of the compatibilizer.

In a following paper, Wanjale and Jog studied the effect of the organic treatment of the clays on the properties of PMP/clay nanocomposites.[65] Three different organically treated clays were used for this study. The microstucture of the nanocomposites was elucidated using XRD. It was observed that the octadecyl amine (ODA)-treated clay showed better thermomechanical properties than the tallow-modified clays. This was attributed to the better dispersion of the clay layers in the ODA-treated clay compared with the tallow-treated clays.

### 13.6.2 Poly(1-butene)/clay nanocomposites

Poly(1-butene) (PB) is a semicrystalline PO with some outstanding mechanical properties, viz. excellent resistance to creep and environmental cracking. It also exhibits time-dependent polymorphism. Wanjale and Jog were first to report the formation and properties of PB/clay nanocomposites.[66, 67] The nanocomposites were characterized for structural and thermomechanical properties using XRD, DMA and TGA. The effect of clay modification on the crystallization behavior of PB and on its solid state transformations was also investigated. The nanocomposites showed an intercalated structure as evidenced from XRD studies. They exhibited improved thermal stability, increased storage modulus and a notable decrease in the coefficient of thermal expansion. The nanocomposites showed enhanced rate of isothermal crystallization compared with the pristine polymer. The most interesting observation made by the authors was the transformation of the metastable tetragonal form to a stable hexagonal form of the nanocomposite at a faster rate than the pristine polymer. They concluded that the observed changes in the properties of PB in PB/clay nanocomposites could be due to the higher aspect ratio of the clay particles and the extent of percolation as a result of intercalation of the polymer in the clay interlayers.

### 13.6.3 Other polyolefin/clay nanocomposites

This section primarily deals with PC nanocomposites prepared from PO copolymers and blends. The commercial importance of polymer blends and copolymers is well known. A few reports involving PC nanocomposites based on these categories of polymers are summarized.

Arroyo *et al*. studied the effect of pristine and organically modified clay

filler on the morphology and tensile properties of PP/LDPE blend matrices using a statistical design.[68] The tensile behavior of the nanocomposites is shown to be more dependent on the matrix composition than on the clay content. A more resistant nanocomposite material is formed from organic modification of clay. A better compatibility between the polymer blend matrix and the clay can be observed from the SEM studies.

Thermal and flammability properties of ethylene–vinyl acetate copolymer (EVA)/clay nanocomposites by blending with LLDPE were reported by Chuang *et al*.[69] Morphological studies revealed the formation of an intercalated nanocomposite structure. An increase in the tensile strength was observed for the addition of 5 parts per hundred resin (phr) of the clay to the EVA/LLDPE blend. The nanocomposite exhibited better protection and stabilization towards thermo-oxidation that is attributed to the barrier diffusion of the volatile decomposition products as well as oxygen from the gas phase to the polymer. The nanocomposite exhibits lower peak heat release rate than the neat polymer blend during combustion. In the presence of conventional fire retardants such as aluminum trihydroxide and antimony trioxide the peak release rate of the nanocomposite is lowered further. The addition of conventional flame retardants to the nanocomposite shows a synergistic effect on the flame retardancy and smoke suppression. Mishra *et al*. reported the preparation and properties of a ternary nanocomposite consisting of LLDPE, millable polyurethane (PU) and organically modified clay.[70] Heat shrink behavior and the mechanical response of this nanocomposite was reported. A decrease in the heat shrinkability as the amount of the clay increased was observed with the entanglement points serving as the memory points during shrinkage. This was attributed to the reduction of the entanglement points in millable PU owing to the presence of the clay that disturbs the entanglement network of the millable PU. The tensile modulus of the nanocomposite increased substantially with increasing amount of clay. Shah *et al*. reported a study on the structure–property relationships for nanocomposites based on a sodium ionomer of poly(ethylene-co-methacrylic acid) and a series of organically modified clays.[71] The presence of surfactant structural aspects that result in more shielding of the silicate surface and the increased alkyl material lead to improved exfoliation in the ionomer.

## 13.7 Conclusions

The results of work on PO/clay nanocomposites are summarized in Table 13.1. The preparation and properties of and issues underlining the structure–property relationships in nanocomposites based on various POs and clays have been systematically reviewed. It was observed that the non-polar nature of POs necessitates the usage of a compatibilizer such as an anhydride or the presence of acidic or ionic groups to improve the matrix polarity. Incorporation

*Table 13.1* Summary of reported work on PO/clay nanocomposites

| Polymer | Clay modifier | Compatibilizer | Method of preparation | Key observations/conclusions | Reference |
|---|---|---|---|---|---|
| PP | Alkyl ammonium cation; octadecyl amine | MA-g-PP | Melt intercalation | Better dispersion of clay.<br>Enhanced crystallization rate.<br>Significant changes in the morphology.<br>Clay layers disturb spherulitic morphology.<br>Enhance mechanical behavior. | 22, 27, 28, 29, 36 |
| | Dioctadecyl-dimethyl ammonium bromide; octadecyl-ammonium bromide | Functionalized PP derivatives | Melt intercalation | Minute amounts of compatibilizer required, thus resemble neat PP closely. | 38 |
| | Semi-fluorinated surfactants | | Melt intercalation | Better mechanical, thermal and solvent resistance. | 38 |
| | Octadecyl and dioctadecyl ammonium salts | Ammonium terminated PP | Physical mixing and melt blending | Exfoliated nanocomposite. | 39 |
| | Amine complexes | | *In situ* polymerization | Mild polymerization conditions.<br>Improved mechanical performance and processability without usage of external activators. | 40 |
| | | MA-g-PP and octadecyl terimethyl ammonium chloride | Melt extrusion | Uniform dispersion of clay.<br>Elimination of organic modification of clay hence cost effective. | 41 |

*Table 13.1* Continued

| Polymer | Clay modifier | Compatibilizer | Method of preparation | Key observations/conclusions | Reference |
|---|---|---|---|---|---|
| | Dimethyl bis(hydrogenated) tallow ammonium chloride; bis(2-hydroxy-ethyl) methyl tallow ammonium chloride | MA | Melt blending | Increased flammability resistance. | 43, 44 |
| | Dimethyl bis(hydrogenated tallow) ammonium chloride; bis(2-hydroxy-ethyl) methyl tallow ammonium chloride | MA-g-PP oligomer | Melt blending | Thermal properties are dependent not only on type of alkyl ammonium surfactant but also on clay interlayer structure. | 45 |
| | Dimethyl bis(hydrogenated) tallow ammonium chloride; octadecyl amine | MA-g-PP | Melt blending | Solid-like rheological response arises due to frictional interactions between clay layers.<br>Threshold concentration of MAPP governs the formation of a percolated network.<br>First direct evidence of flow-induced orientation of clay tactoids.<br>Strain-induced hardening and rheopexy originate from the perpendicular alignment of clay layers to the stretching direction. | 47, 48, 49 50 |

| | | | | | |
|---|---|---|---|---|---|
| LDPE | Octadecyl amine | Ultra-low density PE-g-MA | Melt mixing | Improved thermal stability.<br>Higher levels of compatibilizer lead to increased elongation of the nanocomposite.<br>Mechanical performance is governed by clay exfoliation and content as well as by amount of compatibilizer.<br>MA-g-LDPE toughens the polymer matrix. | 51 |
| LLDPE | Dimethyldistearyl ammonium; dimethylstearylbenzyl ammonium salts | | *In situ* polymerization; melt compounding | Metallocene catalyzed *in situ* polymerization proved more effective than melt compounding in nanocomposite preparation. | 53 |
| | Dimethyl dihydrogenated tallow ammonium chloride; octadecyl amine | MA modified PE | Melt compounding | Hydrophobicity of the modified clay and hydrophilicity of maleated PE govern the morphology of the nanocomposite. | 54 |
| | Dimethyl dihydrogenated tallow ammonium chloride | Zinc-neutralized carboxalate ionomer. MA | Melt blending | Mechanical performance of nanocomposites with ionomer is only slightly below that of nanocomposites with MA. | 55 |
| | Octadecyl amine | MA-g-LLDPE oligomer | Melt compounding | Nanocomposites were prepared from metallocene and Ziegler–Natta catalyzed LLDPE.<br>The former was found to be more effective in exfoliating the clay layers than the latter. | 56 |

*Table 13.1* Continued

| Polymer | Clay modifier | Compatibilizer | Method of preparation | Key observations/conclusions | Reference |
|---|---|---|---|---|---|
| | Dimethyl bis(hydrogenated) tallow ammonium chloride; trimethyl hydrogenated tallow ammonium salt | LLDPE-g-MA | Melt compounding | Modifier with two alkyl tails found to be better than that with one tail. | 57 |
| HDPE | Quaternary ammonium salt | Maleated PE | Melt compounding | Lamellae not chains govern the final orientation of polymer crystals. | 58 |
| | Octadecyltrimethyl ammonium; dioctadecyldimethyl ammonium; benzylhexadecyl-trimethyl ammonium; tributyloctadecyl phosphonium; triphenylhexadecyl phosphonium | | Melt blending | Reduces the polymer permeability coefficient.<br>Gas permeability strongly dependent on average aspect ratio of the fillers. | 59, 60 |
| | Octadecyl trimethyl ammonium salt | Acrylic acid | Melt compounding | Enhanced mechanical performance. Decrease in melting temperature and degree of crystallization of the matrix. | 61 |
| | Dimethyl dialkyl ammonium salt | | Melt processing | Primary mechanism of deformation in nanocomposites is altered from combination of craze and drawing | 62 |

| | | | | | |
|---|---|---|---|---|---|
| | | | | of fibrils of HDPE to microvoid–coalescence–fibrillation process. | |
| UHMWPE | | | Melt intercalation | Better thermomechanical properties. | 63 |
| PMP | Dimethyl hydrogenated tallow 2-ethylhexyl-quaternary ammonium methyl sulfate; dimethyl dihydrogenated tallow ammonium chloride | PE-MA-acrylic ester terpolymer | Melt blending | Compatibilizer with high softening/melting point governs the properties of nanocomposites. | 64 |
| | Octadecyl amine; dimethyl hydrogenated 2-ethylhexyl quaternary ammonium methyl sulfate; quaternary ammonium methyl sulfate; | | Melt blending | Enhanced mechanical performance. | 65 |
| PB | Octadecyl amine | | Melt blending | Enhanced thermomechanical properties.<br>Faster transformation of the metastable tetragonal form to a stable hexagonal form. | 66, 67 |
| PP/LLDPE | Alkylbenzene dimethyl ammonium chloride | | Melt blending | Tensile behavior depended on matrix composition rather than clay content. | 68 |

*Table 13.1* Continued

| Polymer | Clay modifier | Compatibilizer | Method of preparation | Key observations/conclusions | Reference |
|---|---|---|---|---|---|
| EVA/LLDPE | Organic modifier contained an allyl group and a lauryl group and two hydroxyethyl groups | | Melt blending | Nanocomposites exhibit lower peak heat release rate. Synergistic effect on fire retardancy and smoke suppressing after addition of conventional fire retardants. | 69 |
| LLDPE/PU | Bis(2-hydroxy-ethyl) methyl tallow ammonium chloride | | Melt blending | Decrease in heat shrinkability with increasing clay content. Enhanced mechanical properties. | 70 |

of suitable functional groups is also found to be beneficial for PO/clay nanocomposite production. Thus by using a suitable combination of compatibilizer and organic modification of clay, PO/clay nanocomposites having superior properties can be fabricated. These nanocomposites possess several advantageous properties, including the following:

- Superior mechanical properties in both solid and melt state compared with the pristine PO as well as conventional filler reinforced POs due to the reinforcing effect of clay at the nano-scale.
- Microstructural properties such as morphology, rate of crystallization and the crystallinity of the PO are greatly affected by the presence of clay layers. Transformation to commercially useful stable polymorphic forms in the presence of clay has been observed in POs that exhibit polymorphism.
- Dramatic improvement is observed in the barrier properties of the PO/clay nanocomposites due to the formation of tortuous paths in the presence of the clay.
- Thermal properties and flame retardancy of the POs in the presence of clays improve due to such phenomena as building up of high-performance carbonaceous–silicate char on the surface during burning, which insulates the underlying material and slows down the mass loss rate of decomposition products.

Intercalation of the polymer chains in the clay interlayer and dispersion level of the clay platelets in the polymer matrix are some of the aspects that govern the properties of these PO/clay nanocomposites. The remarkable property improvement at low filler loadings makes these nanocomposites an attractive choice for the development of materials with fascinating properties and a rich variety of applications. Although much has been reported on the various aspects of preparation and property enhancements in PO/clay nanocomposites, a more in-depth understanding of the structure–property relationships in these nanocomposites is essential for the total utilization of their complete commercial potential. Only then can PO/clay nanocomposites truly be termed modern 'high-performance commodity plastics'.

## 13.8 References

1. Kurauchi T., Okada A., Nomura T., Nishio T., Saegusa S. and Deguchi R., 'Nylon 6–clay hybrid – synthesis, properties and application to automotive timing belt cover', *SAE Technical Paper Series 910584,* International Congress and Exposition, Detroit, 1991.
2. Bailey S. W., 'The status of clay mineral structures', *Clay and Clays Minerals Proc 14th National Conference*, Berkley, California, Pergamon Press, 1966.
3. Greenland D. J., Laby R. H. and Quirk J. P., 'Adsorption of amino-acids and peptides by montmorillonite and illite. Part 1. Cation exchange and proton transfer', *Trans Faraday Soc*, 1965, **61**, 2013–2023.

4. Van Olphen H., *An Introduction to Clay Colloids Chemistry*, New York, John Wiley and Sons Inc, 1977.
5. Hendricks S. B., 'Base exchange of the clay mineral montmorillonite for organic cations and its dependence upon adsorption due to Van der Waals forces', *J Phys Chem*, 1941, **45**, 65–81.
6. Grim R. E., Allaway W. H. and Cuthbert F. L., 'Reaction of different clay minerals with some organic cations', *J Am Ceram Soc*, 1947, **30**, 137–142.
7. Cowan C. T. and White D., 'The mechanism of exchange reactions occurring between sodium montmorillonite and various *n*-primary aliphatic amine salts', *Trans Faraday Soc*, 1958, **54**, 691–697.
8. Vansant E. F. and Uytterhoeven J. B., 'Thermodynamics of the exchange of *n*-alkylammonium ions on sodium–montmorillonite', *Clay Clay Miner*, 1972, **20**, 47–54.
9. Barrer R. M. and Brummer K., 'Relations between partial ion exchange and interlamellar sorption in alkylammonium montmorillonite', *Trans Faraday Soc*, 1963, **59**, 959–968.
10. Greenland D. J., 'Interactions between clays and organic compounds in soils', *Soils Fertilizers*, 1965, **28**, 415–425.
11. Jordan J. W., 'Organophilic bentonites I. Swelling in organic liquids', *J Phys Colloid Chem*, 1949, **53**, 294–306.
12. Jordan J. W., Hook B. J. and Finlayson C. M., 'Organophilic bentonites II' *J Phys Colloid Chem*, 1950, **54**, 1196–1208.
13. Greene-Kelly R., 'Sorption of aromatic organic compounds by montmorillonite. Part 1. – orientation studies', *Trans Faraday Soc*, 1955, **51**, 412–424.
14. Lagaly G., 'Interaction of alkylamines with different types of layered compounds', *Solid State Ionics*, 1986, **22**, 43–51.
15. Hackett E., Manias E. and Giannelis E. P., 'Molecular dynamics simulations of organically modified layered silicates', *J Chem Phys*, 1998, **108**, 7410–7415.
16. Kornmann X., Lindberg H. and Berglund L. A., 'Synthesis of epoxy–clay nanocomposites: influence of the nature of the clay on the structure', *Polymer*, 2001, **42**, 1303–1310.
17. Messersmith P. B. and Giannelis E. P., 'Synthesis and characterization of layered silicate–epoxy nanocomposites', *Chem Mater*, 1994, **6**, 1719–1725.
18. Kornmann X., Lindberg H. and Berglund L. A., 'Synthesis of epoxy–clay nanocomposites: influence of the nature of the curing agent on the structure', *Polymer*, 2001, **42**, 4493–4499.
19. Kurokawa Y., Yasuda H., Kashiwagi M. and Oya A., 'Structure and properties of a montmorillonite/polypropylene nanocomposite', *J Mater Sci Lett*, 1997, **16**, 1670–1672.
20. Kawasumi M., Hasegawa N., Kato M., Usuki A. and Okada A., 'Preparation and mechanical properties of polypropylene–clay hybrids', *Macromolecules*, 1997, **30**, 6333–6338.
21. Kato M., Usuki A. and Okada A., 'Synthesis of polypropylene oligomer–clay intercalation compounds', *J Appl Polym Sci*, 1997, **66**, 1781–1785.
22. Hasegawa N., Kawasumi M., Kato M., Usuki A. and Okada A., 'Preparation and mechanical properties of polypropylene–clay hybrids using a maleic anhydride–modified polypropylene oligomer', *J Appl Polym Sci*, 1998, **67**, 87–92.
23. Oya A., Kurokawa Y. and Yasuda H., 'Factors controlling mechanical properties of clay mineral/polypropylene nanocomposites', *J Mater Sci*, 2000, **35**, 1045–1050.

24. Reichert P., Nitz H., Klinke S., Brandsch R., Thomann R. and Mulhaupt R., 'Poly(propylene)/organoclay nanocomposite formation: influence of compatibilizer functionality and organoclay modification', *Macromol Mater Eng*, 2000, **275**, 8–17.
25. Ishida H., Campbell S. and Blackwell J., 'General approach to nanocomposite preparation', *Chem Mater*, 2000, **12**, 1260–1267.
26. Wang H., Zeng C., Svoboda P. and James Lee L., 'Preparation and properties of polypropylene nanocomposites', *59th ANTEC Proceedings*, Dallas, 2001, 2203–2207.
27. Kodgire P., Kalgaonkar R., Hambir S., Bulakh N. and Jog J. P., 'PP/clay nanocomposites: effect of clay treatment on morphology and dynamic mechanical properties', *J Appl Polym Sci*, 2001, **81**, 1786–1792.
28. Hambir S., Bulakh N., Kodgire P., Kalgaonkar R. and Jog J. P., 'PP/clay nanocomposites: a study of crystallization and dynamic mechanical behavior', *J Polym Sci Part B: Polym Phys*, 2001, **39**, 446–450.
29. Hambir S., Bulakh N. and Jog J. P., Polypropylene/clay nanocomposites: effect of compatibilizer on thermal, crystallization and dynamic mechanical behavior', *Polym Eng Sci*, 2002, **42**, 1800–1807.
30. Kim K.-N., Kim H. and Lee J.-W., 'Effect of interlayer structure, matrix viscosity, and composition of a functionalized polymer on the phase structure of polypropylene–montmorillonite nanocomposites', *Polym Eng Sci*, 2001, **41**, 1963–1969.
31. Szazdi L., Pukanszky Jr B., Foldes E. and Pukanszky B., 'Possible mechanism of interaction among the components in MAPP modified layered silicate PP nanocomposites', *Polymer*, 2005, **46**, 8001–8010.
32. Wang Y., Chen F.-B., Li Y.-C. and Wu K.-C., 'Melt processing of polypropylene/clay nanocomposites modified with maleated polypropylene compatibilizers', *Compos Part B – Eng*, 2004, **35**, 111–124.
33. Garcia-Lopez D., Picazo O., Merino J. C. and Pastor J. M., 'Polypropylene–clay nanocomposites: effect of compatibilizing agents on clay dispersion', *Eur Polym J*, 2003, **39**, 945–950.
34. Ding C., Jia D., He H., Guo B. and Hong H., 'How organo–montmorillonite truly affects the structure and properties of polypropylene', *Polym Test*, 2005, **24**, 94–100.
35. Usuki A., Kato M., Okada A. and Kurauchi T., 'Synthesis of polypropylene–clay hybrid', *J Appl Polym Sci*, 1997, **63**, 137–139.
36. Hasegawa N., Okamoto H., Kato M. and Usuki A., 'Preparation and mechanical properties of polypropylene–clay hybrids based on modified polypropylene and organophilic clay', *J Appl Polym Sci*, 2000, **78**, 1918–1922.
37. Vaia R. A. and Giannelis E. P., 'Lattice model of polymer melt intercalation in organically-modified layered silicates', *Macromolecules*, 1997, **30**, 7990–7999.
38. Manias E., Touny A., Wu L., Lu B., Strawhecker K., Gilman J. W., and Chung T. C., 'Polypropylene/montmorillonite nanocomposites. Review of the synthetic routes and material properties', *Chem Mater*, 2001, **13**, 3516–3523.
39. Wang, Z. M., Nakajima, H., Manias, E. and Chung T. C., 'Exfoliated PP/clay nanocomposites using ammonium-terminated PP as the organic modification for montmorillonite', *Macromolecules*, 2003, **36**, 8919–8922.
40. Sun T. and Garces J. M., 'High-performance polypropylene–clay nanocomposites by *in-situ* polymerization of metallocene/clay catalysts', *Adv Mater*, 2002, **14**, 128–130.
41. Kato M., Matsushita M. and Fukumori K., 'Development of new production method for a poypropylene–clay nanocomposite', *Polymer Nanocomposites 2003, International*

*Symposium on Polymer Nanocomposites Science and Technology*, Quebec, Canada, 2003.
42. Zhao Z., Tang T., Qin Y. and Huang B., 'Effects of surfactant loadings on the dispersion of clays in maleated polypropylene', *Langmuir*, 2003, **19**, 7157–7159.
43. Gilman J. W., Jackson C. L., Morgan A. B., Harris R., Manias E., Giannelis E. P., Wuthenow M., Hilton D. and Philips S. H., 'Flammability properties of polymer-layered–silicate nanocomposites. Polypropylene and polystyrene nanocomposites', *Chem Mater*, 2000, **12**, 1866–1873.
44. Zanetti M., Camino G., Canavese D., Morgan A. B., Lamelas F. J. and Wilkie C. A., 'Fire retardant halogen–antimony–clay synergism in polypropylene layered silicate nanocomposites', *Chem Mater*, 2002, **14**, 189–193.
45. Lee J. W., Lim Y. T. and Park O. O., 'Thermal characteristics of organoclay and their effects upon the formation of polypropylene/organoclay nanocomposites', *Polym Bull*, 2000, **45**, 191–198.
46. Maiti P., Nam P. H., Okamoto M., Hasegawa N. and Usuki A., 'Influence of crystallization on intercalation, morphology, and mechanical properties of polypropylene/clay nanocomposites', *Macromolecules*, 2002, **35**, 2042–2049.
47. Galgali G., Ramesh C. and Lele A., 'Rheological study on the kinetics of hybrid formation in polypropylene nanocomposites', *Macromolecules*, 2001, **34**, 852–858.
48. Abranyi A., Szazdi L., Pukanszky Jr B., Vancso G. J. and Pukanszky B., 'Formation and detection of clay network structure in poly(propylene)/layered silicate nanocomposites', *Macromol Rapid Commun*, 2006, **27**, 132–135.
49. Lele A., Mackley M., Galgali G. and Ramesh C., '*In situ* rheo-X-ray investigation of flow-induced orientation in layered silicate–syndiotactic polypropylene nanocomposite melt', *J Rheol*, 2002, **46**, 1091–1110.
50. Okamoto M., Nam P. H., Maiti P., Kotaka T., Hasegawa N. and Usuki A., 'A house of cards structure in polypropylene/clay nanocomposites under elongational flow', *Nano Lett*, 2001, **1**, 295–298.
51. Morawiec J., Pawlak A., Slouf M., Galeski A., Piorkowska E. and Krasnikowa N., 'Preparation and properties of LDPE/organo-modified montmorillonite nanocomposites', *Eur Polym J*, 2005, **41**, 1115–1122.
52. Antipov E. M., Guseva M. A., Gerasin V. A., Korlev, Yu M., Rebrov A. V., Fischer H. R. and Razumovskaya I. V., 'Structure and deformation behavior of nanocomposites based on LDPE and modified clays', *Polym Sci Ser A*, 2003, **45**, 1130–1139.
53. Heinemann J., Reichert P., Thomann R. and Mulhaupt R., 'Polyolefin nanocomposites formed by melt compounding and transition metal catalyzed ethane homo- and copolymerization in presence of layered silicates', *Macromol Rapid Commun*, 1999, **20**, 423–430.
54. Wang K. H., Choi M. H., Koo C. M., Choi Y. S. and Chung I. J., 'Synthesis and characterization of maleated polyethylene/clay nanocomposites', *Polymer*, 2001, **42**, 9819–9826.
55. Sanchez-Valdes S., Lopez-Quintanilla M. L., Ramirez-Vargas E., Medellin-Rodriguez F. J. and Gutierrez-Rodriguez J. M., 'Effect of ionomeric compatibilizer on clay dispersion in polyethylene/clay nanocomposites', *Macromol Mater Eng*, 2006, **291**, 128–136.
56. Lew C. Y., Murphy W. R. and McNally G. M., 'Preparation and properties of polyolefin-clay nanocomposites', *Polym Eng Sci*, 2004, **44**, 1027–1035.
57. Hotta S. and Paul D. R., 'Nanocomposites formed from linear low density polyethylene and organoclays', *Polymer*, 2004, **45**, 7639–7654.

58. Bafna A., Beaucage G., Merabella F. and Mehta S., '3D hierarchical orientation in polymer–clay nanocomposite films', *Polymer*, 2003, **44**, 1103–1115.
59. Osman M. A. and Atallah A., 'High-density polyethylene micro- and nanocomposites: effect of particle shape, size, and surface treatment on polymer crystallinity and gas permeability', *Macromol Rapid Commun*, 2004, **25**, 1540–1544.
60. Osman M. A., Rupp J. E. P. and Suter U. W., 'Gas permeation properties of polyethylene-layered silicate nanocomposites', *J Mater Chem*, 2005, **15**, 1298–1304.
61. Xu Y., Fang Z. and Tong L., 'On promoting intercalation and exfoliation of bentonite in high-density polyethylene by grafting acrylic acid', *J Appl Polym Sci*, 2005, **96**, 2429-2434.
62. Tanniru M., Yuan Q. and Misra R. D. K., 'On significant retention of impact strength in clay-reinforced high-density polyethylene (HDPE) nanocomposites', *Polymer*, 2006, **47**, 2133–2146.
63. Park S.-J., Li K. and Hong S.-K., 'Preparation and characterization of layered silicate-modified ultrahigh-molecular-weight polyethylene nanocomposites', *J Ind Eng Chem*, 2005, **11**, 561–566.
64. Wanjale S. D. and Jog J. P., 'Effect of modified layered silicates and compatibilizer on properties of PMP/clay nanocomposites', *J Appl Polym Sci*, 2003, **90**, 3233–3238.
65. Wanjale S. D. and Jog J. P., 'Poly(4-methyl-1-pentene) nanocomposites: effect of organically modified layered silicates', *Polym Int*, 2003, **53**, 101–105.
66. Wanjale S. D. and Jog J. P., 'Poly(1-butene)/clay nanocomposites: preparation and properties', *J Polym Sci Part B: Polym Phys*, 2003, **41**, 1014–1021.
67. Wanjale S. D. and Jog J. P., 'Poly(1-butene)/clay nanocomposites: a crystallization study', *J Macromol Sci*, 2003, **B42**, 1141–1152.
68. Arroyo M., Suarez R. V., Herrero B. and Lopez-Manchado M. A., 'Optimization of nanocomposites based on polypropylene/polyethylene blends and organo-bentonite', *J Mater Chem*, 2003, **13**, 2915–2921.
69. Chuang T.-H., Guo W., Cheng K.-C., Chen S.-W., Wang H.-T. and Yen Y.-Y., 'Thermal properties and flammability of ethylene–vinyl acetate copolymer/montmorillonite/polyethylene nanocomposites with flame retardants', *J Polym Res*, 2004, **11**, 169–174.
70. Mishra J. K., Kim I. and Ha C., 'Heat shrinkable behavior and mechanical response of a low-density polyethylene/millable polyurethane/organoclay ternary nanocomposite', *Macromol Rapid Commun*, 2004, **25**, 1851–1855.
71. Shah R. K., Hunter D. L. and Paul D. R., 'Nanocomposites from poly(ethylene-co-methacrylic acid) ionomers: effect of surfactant structure on morphology and properties', *Polymer*, 2005, **46**, 2646–2662.

# 14

# Multiwall carbon nanotube–nylon-6 nanocomposites from polymerization

Y. K. KIM and P. K. PATRA, University of Massachusetts Dartmouth, USA

## 14.1 Introduction

Since their discovery in the early 1990s[1] carbon nanotubes (CNTs) have excited scientists and engineers with their wide range of unusual physical properties. Typical features of the carbon nanotubes are: extremely small size (diameter from 1 to 40 nm and length around few micrometers), excellent mechanical properties (elastic modulus around 1 TPa, strength around 30 GPa and fracture strains about 20%), novel electric properties i.e. from perfect electric conductors (resistivity around $10^{-4}$ Ω cm and current density as high as 109 A/cm$^2$) to semiconductors and high thermal conductivity.[2–10] To take advantage of this unique combination of size and properties, a wide variety of applications have been proposed for carbon nanotubes, including: chemical and genetic probes, batteries, fuel cells, fibers, cables, pharmaceutics and biomedical materials, field emission tips, mechanical memory, supersensitive sensors, hydrogen and ion storage, scanning probe microscope tips and structural materials.[11]

Owing to small production quantities in the past, research to date has concentrated on small-volume applications (electronics, sensors, etc.). However, worldwide development in synthesis of large-scale single wall carbon nanotubes (SWNTs) and multiwall carbon nanotubes (MWNTs), has encouraged research in the use of carbon nanotubes in composites. Carbon nanotube-based composites have the potential to revolutionize structural materials for aerospace, electrical and thermal conductors for energy applications, nano-biotechnology and other disciplines.[3]

Nanotubes are a very attractive reinforcing material for polymer composite structures. Their extremely high aspect ratio and their amazingly high modulus and strength are the main reasons for so many studies that are conducted in the polymer–nanotubes composites field. An extremely high elastic modulus and strain to failure coupled with a tensile strength an order of magnitude higher than conventional carbon fibers, qualify carbon nanotubes especially as the ultimate reinforcement in polymer composite materials.

There are however three main problems in successful preparation of carbon nanotube-based nanocomposites. These are dispersion, orientation of carbon nanotubes and adhesion between carbon nanotubes and matrix.[12] In this research work, MWNT–nylon-6 nanocomposites were prepared using the *in situ* polymerization technique (ring opening polymerization of ε-caprolactam to form nylon-6 polymer in the presence of carbon nanotubes), assisted by a few minutes (4 min) of ultrasonication. Micrometer-sized fibers were then extruded from prepared nanocomposite using a single screw extruder. The prepared fibers were characterized for the dispersion and orientation of carbon nanotubes using scanning electron microscopy (SEM), non-isothermal crystallization studies using differential scanning calorimetry (DSC) and mechanical properties using Instron. The dilute solution viscometry and simple theoretical models of filled polymers were used to approximately determine the effect of the MWNTs on the molecular weight of the prepared nylon-6 polymer.

## 14.2 Nanocomposite synthesis and production

### 14.2.1 Materials

- ε-Caprolactam (Fisher Scientific).
- Sodium hydride (NaH), 60% dispersion in oil (Fisher Scientific).
- Polyoxyethylene (POE), MW = 6000 g/moles (Fisher Scientific).
- *N*-acetylcaprolactam ( Fisher Scientific).
- Multiwall carbon nanotubes (0.5% and 1% on weight of polymer) (Catalytic Materials, Holliston, MA).

### 14.2.2 Equipment

- Glass beaker.
- Balance.
- Cole Parmer Ultrasonic Processor 750 Watts.

### 14.2.3 Synthesis procedure

- ε-Caprolactam (40 g), polyoxyethylene (0.88 g) carbon nanotubes (0.5%, 1% on weight of polymer) and *N*-acetylcaprolactam (20 drops) were placed in a beaker.
- The mixture in the beaker was heated slowly using a Bunsen burner.
- The molten solution was subjected to 4 min ultrasonication (Cole Parmer Ultrasonic Processor 750 W. Parameters – 80% amplitude, 5 s on, 5 s off) to break the agglomerations of carbon nanotubes.
- NaH (0.15 g) was added when the mixture in the tube melted.

- Heating continued for 4–6 min until the reaction mixture became much more viscous.
- Thin films of prepared nanocomposite were made using a hot press (230 °C and 30 s pressing time). Thin films were cut into pieces and washed with hot water to remove any unreacted species present in the polymer.

### 14.2.4 Carbon nanotube/nylon-6 composite fiber production

The cut pieces of the nylon polymer and composites were placed in a Cole Parmer vacuum oven at 70 °C for 24 h to remove water and moisture contents. Neat nylon-6 and nanocomposite fibers were prepared using a Brabender single screw extruder (Intelli-torque) and single hole fiber die (diameter = 0.016 inches (0.4 mm), *L*/*D* ratio = 4) with the following parameters:

- Temperature zone 1 = 250 °C.
- Temperature zone 2 = 230 °C.
- Temperature zone 3 = 230 °C.
- Screw speed = 3.

The extruded fibers were allowed to fall freely without any tension and then wound on bobbins. The extruded fibers were stretched with draw ratios 3 and 4 using Instron fiber clamps at room temperature. Stretched samples were used for further characterization.

## 14.3 Characterization techniques

### 14.3.1 Scanning electron microscopy analysis

SEM studies were done on the cross-sectional surfaces of the broken fibers to study the dispersion and orientation of the carbon nanotubes in the fibers. The fibers were clamped vertically using Scotch tape and adhesive onto SEM stubs. The stubs and the samples were coated with gold using a Denton Vacuum Desk-II sputtering machine. The cross-sectional surfaces of the broken fibers were observed under different magnification levels using a JEOL JSM-5610 high vacuum scanning electron microscope.

Intrinsic viscosities of nylon-6 polymer and nanocomposites were determined using dilute solution viscometry (ASTM D2857-95). Efflux times for 40% sulfuric acid and different concentrations of nylon-6 polymer and nanocomposite solutions were determined using a Ubbelohde-type viscometer. Four concentrations were prepared for each sample. The efflux time values were used further to determine the various terms listed in Table. 14.1, which shows the definition of the terms used in dilute solution viscometry, where

*Table 14.1* Definition of different terms used in dilute solution viscometry

| Common name | Name proposed by IUPAC | Symbol and definition |
|---|---|---|
| Relative viscosity | Viscosity ratio | $\eta_{rel} = \frac{\eta}{\eta_0} = \frac{t}{t_0}$ |
| Specific viscosity | | $\eta_{sp} = \eta_{rel} - 1$ |
| Reduced viscosity | Viscosity number | $\eta_{red} = \eta_{sp}/c$ |
| Inherent viscosity | Logarithmic viscosity number | $\eta_{inh} = \ln(\eta_{rel})/c$ |
| Intrinsic viscosity | Limiting viscosity number | $[\eta] = \lim_{c \to 0} (\eta_{red})$ |

$t_0$ and $t$ are the efflux times for solvent and polymer solution respectively and $c$ is concentration of solution in g/dl or g/ml.

Viscosity average molecular weight for nylon-6 polymer was determined using the intrinsic viscosity and the Mark–Houwink equation.

$$[\eta]\ KM^a \qquad [14.1]$$

where $[\eta]$ = intrinsic viscosity
$a$ and $K$ = Mark–Houwink constants
$M$ = polymer molecular weight
$a = 0.69$ and $K = 59.2 \times 10^{-03}$ ml/g for nylon-6 and 40% $H_2SO_4$.[13]

In order to determine the molecular weight of nylon-6 polymer in the nanocomposite, it was assumed that the viscosity of nanocomposite solution had been altered by the carbon nanotubes according to the theory of dilute Brownian rods.[14, 15] The intrinsic viscosity of nylon-6 polymer in the nanocomposite was determined by excluding the effect of carbon nanotubes:[14, 15]

$$\frac{\eta - \eta_s}{\eta_s \phi} = \frac{2(L/R)^2}{45[\ln (L/R)]} \left[ \left( \frac{1 + \frac{0.64}{\ln (L/R)}}{1 - \frac{1.5}{\ln (L/R)}} \right) + \frac{1.659}{(\ln (L/R))^2} \right] \qquad [14.2]$$

where $\eta$ = viscosity of solution
$\eta_s$ = viscosity of suspension
$L$ = length of rods (fillers)
$R$ = radius of rods
$\phi$ = volume fraction of rods

Viscosity-average molecular weight for nylon-6 polymer and the nanocomposite was then determined using the Mark–Houwink equation.

### 14.3.2 Differential scanning calerimetry and non-isothermal crystallization kinetics studies

DSC analysis was performed on the nylon-6 and the nanocomposite samples to understand the effect of the carbon nanotubes on the melting behavior and the percentage crystallinity. The values of melting point and heat of melting were measured during a second heating cycle. Percentage crystallinity was determined using Equation 14.3:

$$\% \text{ Crystallinity} = \frac{\Delta H_s}{\Delta H_c} \times 100 \qquad [14.3]$$

where $\Delta H_s$ = heat of fusion for sample (J/g)
$\Delta H_c$ = heat of fusion for 100% crystalline nylon-6 polymer (J/g) = 230 J/g[13]

Non-isothermal crystallization kinetics for nylon-6 and nanocomposite samples were studied. The onset of the crystallization, crystallization temperature and the heat of the crystallization were noted during the cooling cycle. Using Universal Analysis software, running integration function was performed for crystallization peak in heat flow (J/g) *vs*. time (minutes) plot to get the values of relative crystallinity $X_t$ for different values of time $t$. The time required for the sample to crystallize 50% ($t_{1/2}$) was noted for the nylon-6 and nanocomposite samples. Then the chart of ln [–ln $(1 - X_t)$] *vs*. ln $t$ was plotted. The Avrami equation was used to determine values of $n$ and $k$ from the slopes and the interception of the best fit (Equation 14.4).

$$\ln [-\ln (1 - X_t)] = n \ln t + \ln k \qquad [14.4]$$

where $k$ = growth rate parameter of Avrami equation
$n$ = nucleation parameter of Avrami equation

The following heat–cool–heat sequence was used in DSC and non-isothermal crystallization studies:

1. Equilibrate at 0 °C.
2. Heat to 240 °C at 20 °C/min.
3. Isothermal at 240 °C for 5 min.
4. Cool to 0 °C at –40 °C/min.
5. Heat to 240 °C at 20 °C/min.

### 14.3.3 Tensile testing

Before mechanical testing, the diameter of each Instron sample was measured using a Leica DMRX optical microscope and micrometer scale under 200× magnification with transmission mode illumination. Three readings per sample (middle and at two ends) were taken and an average value was determined.

Mechanical properties were measured using an Instron tensile tester and ASTM standard test procedures – D3822-01.

- Sample conditioning – samples were kept for 24 h in testing laboratory for moisture equilibrium.
- Gauge length – 5 cm.
- Sample preparation – single filament was secured to two cardboard pieces with Quicktite superglue (cynoacrylate-based adhesive by Locktite).
- Extension rate – 60% of initial specimen length/min, or 3 cm/min.
- Sample size – 15 per batch.

The following properties were measured:

- initial modulus (MPa);
- breaking strength (MPa);
- breaking strain (%).

Fifteen samples from different portions of the extruded fibers were used for tensile testing. The linear curve fit equation was determined for the initial part of the stress–strain curve (strain 0–3%) for each sample using Microsoft Excel. The slope of the equation gives the initial modulus. Breaking strength and breaking strain were calculated at the point of maximum load.

## 14.4 Properties of multiwall carbon nanotube–nylon-6 nanocomposite fibers

During *in situ* polymerization we observed that polymerization became much more difficult with increasing wt% of MWNTs. With increasing amount of wt% MWNTs, the time required to build sufficient viscosity increased. For example it took around 2–3 min to polymerize (i.e. attain sufficient viscosity) neat nylon-6, but with 0.5 wt% MWNTs, it took around 4–5 min to attain similar viscosity. This time was increased to about 5 min with 1 wt% MWNTs in the mixture. This shows that the rate of polymerization has been affected by the presence of carbon nanotubes.

With the method used in this work, nanocomposites with more than 1 or 1.5 wt% MWNTs can not be prepared. Some possible reasons for this are as follows:

- Because of the significantly reduced polymerization rate, the time required to build sufficient viscosity increases. As time goes on, the active species (the sodium salt of caprolactam) in the formulation react with moisture in the air, resulting in termination of the growing chains. This results in very low molecular weight nylon-6 polymer.
- With increasing time, the temperature of the formulation goes very high, which results in degradation of the contents.

The very high specific area of the MWNTs plays a major role in reducing the polymerization rate. Assuming a density of about 1.5 g/cm$^3$ and length around 4 μm, MWNTs having a diameter of 30 nm give a surface area of 78 m$^2$/g.

Figure 14.1 shows the SEM image of the cross-section of a broken nanocomposite fiber (0.5 wt% MWNTs). Well-separated MWNTs were observed throughout the cross-section. Carbon nanotubes appear as bright tiny dots in the SEM images due to charging. Figures 14.2 and 14.3 are some additional images of the cross-section and show the well-separated carbon nanotubes. As carbon nanotubes appear as tiny, near-round dots in the cross-section of the fiber it is likely that they are nearly oriented along the direction of the fiber.

### 14.4.1 Mechanism of dispersion

*Viscosity effect*

It is now known that ultrasonication energy can efficiently disperse the carbon nanotubes or nanoparticles in the solutions having low viscosity.[16] In the experiments, the carbon nanotubes were added to a molten monomer solution (ε-caprolactam) having low viscosity, i.e. before polymerization. So a small amount of ultrasonication energy and time are enough to break the agglomerations and disperse carbon nanotubes effectively.

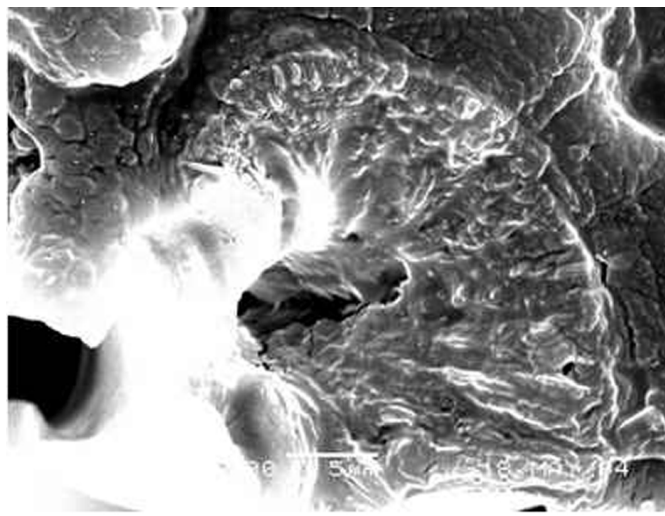

*14.1* Dispersion of MWNTs, SEM image of cross-section of broken fibers (0.5 wt% MWNTs) magnification ×3500.

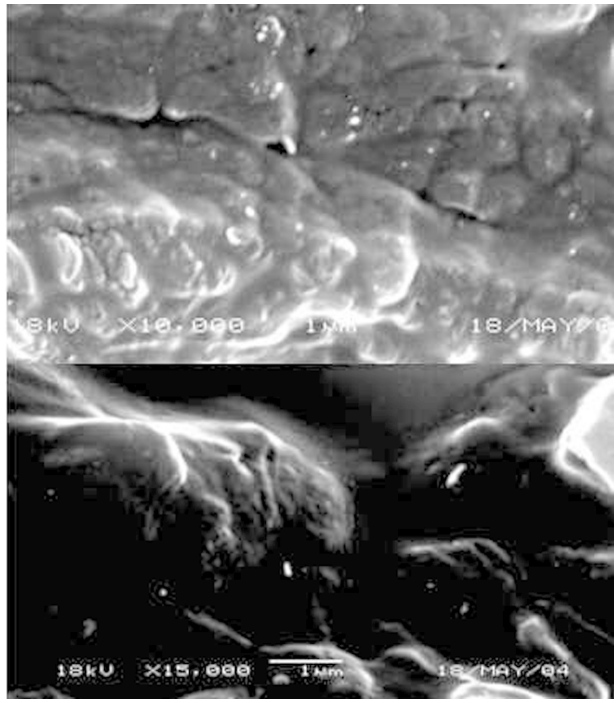


*14.2* Dispersion of MWNTs, SEM image of cross-section of broken fibers (0.5 wt% MWNTs).

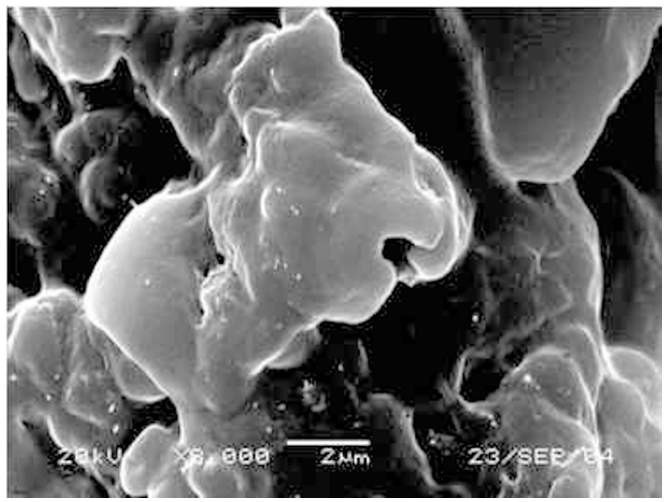


*14.3* Dispersion of MWNTs, SEM image of cross-section of broken fibers (1 wt% MWNTs).

*Time effect*

Re-agglomeration of the carbon nanotubes in the solution is a time-dependent phenomenon.[17] Ultrasonically separated particles tend to agglomerate again after some time. This phenomenon depends upon solvent–nanoparticle interaction, chemical treatment given to nanoparticles (functionalization), presence of dispersing agent or surfactant, viscosity and concentration of particles in solvent. In these experiments, polymerization occurs within a few minutes (2–5 min) after ultrasonication, so polymer chains initiate and propagate between well-separated carbon nanotubes, which lowers the cohesive force of attraction between carbon nanotubes that binds the nanoparticles. This can lead to efficient separation and dispersion of carbon nanotubes. Once the polymerization occurs, because of high viscosity, there is a little chance of getting particles re-agglomerated in further processing such as during fiber extrusion.

*Chain formation effect*

In the *in situ* technique, owing to the random nature of chain propagation and growth of polymeric molecules, the chances are very high that chains will form between individual carbon nanotubes. Use of ultrasonication can also encourage monomer molecules to go very close to the surfaces of a carbon nanotube. It is possible to wrap carbon nanotubes by the polymeric chain, depending on the affinity between the carbon nanotubes and monomer solution. It is also quite possible that monomer $\varepsilon$-caprolactam can penetrate and polymerize inside MWNTs, as it has an inner diameter of about 3–4 nm,[16] which is much larger than molecular size of ε-caprolactam (few angstroms). The mechanism of dispersion is explained in Fig. 14.4.

*Differential scanning calorimetry analysis*

Figure 14.5 shows the DSC curves for the neat nylon-6 and nanocomposite samples (replica 1). The results show that there is no significant effect of the carbon nanotubes on the melting temperature of the composite; however,

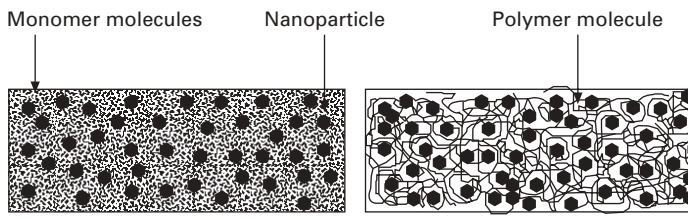


*14.4* Dispersion mechanism in *in situ* polymerization.

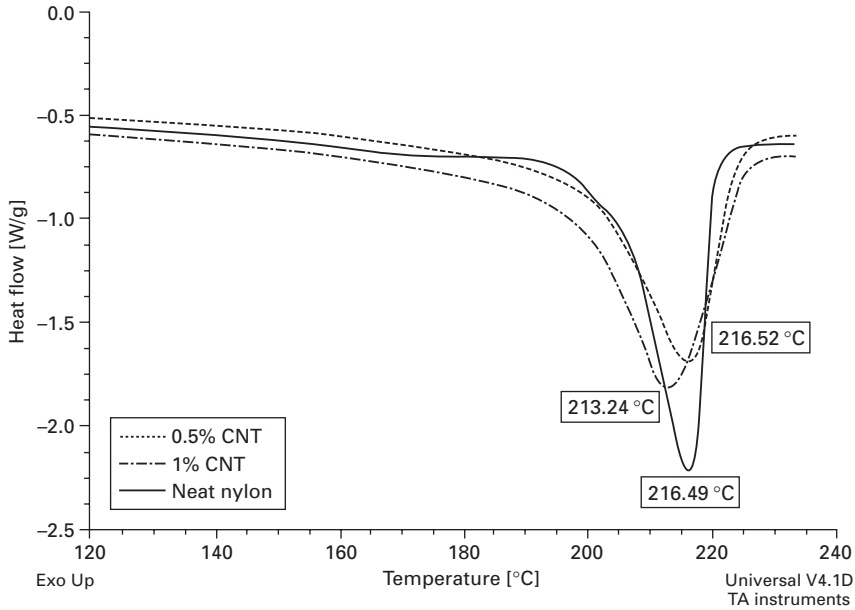


*14.5* DSC melting curves for neat nylon-6 and nanocomposites.

*Table 14.2* Melting characteristics and crystallinity of neat nylon and nanocomposites

| MWNT (wt%) | Melting point (°C) | Heat of fusion (J/g) | Crystallinity (%) |
|---|---|---|---|
| 0 | 216 | 52 | 23 |
| 0.5 | 217 | 60 | 26 |
| 1 | 214 | 69 | 30 |

nanocomposites show higher crystallinity than neat nylon-6. An increase in crystallinity of 15% was observed for 0.5 wt% MWNT and 32% for 1 wt% MWNT nanocomposite (Table 14.2). It is important to note that neat nylon-6 shows a narrow melting peak, whereas nanocomposites show a broad melting peak. Figure 14.5 also shows a big difference in onset of melting. The broad peak and early onset of melting suggest the presence of smaller and defective crystals in the nanocomposites. It is quite possible that MWNTs obstruct or interfere with the growth of crystals around them and makes them smaller, defective or both. The increase in crystallinity can be attributed to the reduced molecular weight, which was observed in dilute solution viscometry experiments. Shorter chains can align more easily during the formation and growth of the crystals. Neat nylon-6 shows a small pre-melting peak which is indication of re-crystallization or reorganization of nylon-6 molecules. Such peaks were absent in the case of nanocomposite samples.

Table 14.2 shows the melting characteristics (average) of neat nylon-6 and nanocomposite samples.

## 14.4.2 Melting characteristics and crystallization

The crystallization exotherms of neat nylon-6 and nanocomposite samples (replica 1) are presented in Fig. 14.6. All the samples were subjected to the same heating profile. Crystallization in nanocomposites starts earlier (about 1 min earlier) or at higher temperature (about 25 °C higher) compared with neat nylon-6 samples. This indicates that carbon nanotubes act as nucleating agents at the early stages of crystallization.

Table 14.3 shows the average crystallization characteristics of neat nylon-6 and nanocomposite samples. The results show that carbon nanotubes

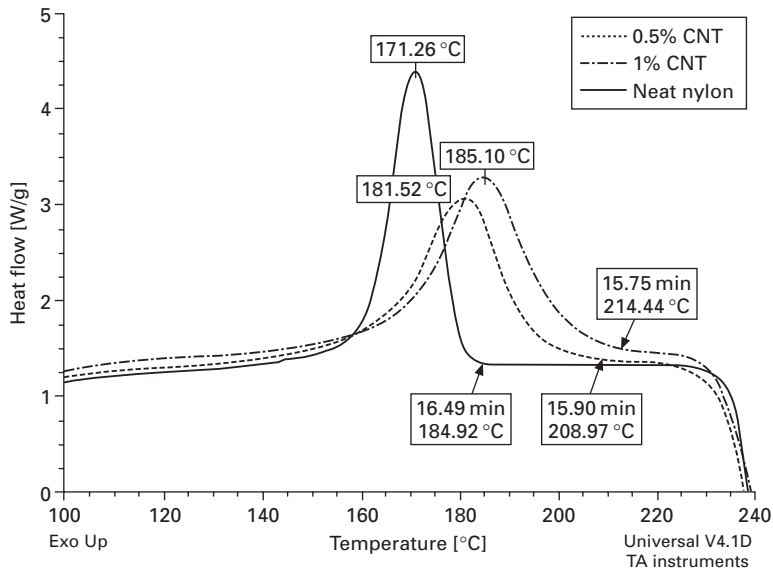


*14.6* DSC crystallization curves for neat nylon-6 and nanocomposites.

*Table 14.3* Crystallization behavior of neat nylon-6 and nanocomposite sample

| | Crystallization start time (min) | Crystallization onset temperature (°C) | Heat of crystallization (J/g) | Crystallization peak temperature (°C) |
|---|---|---|---|---|
| Neat nylon | 16.49 | 185 | 60 | 170 |
| 0.5 wt% MWNT | 15.91 | 208 | 56 | 182 |
| 1 wt% MWNT | 15.79 | 213 | 62 | 185 |

significantly alter the crystallization behavior of the nylon-6 polymer. Nanocomposite samples show higher heat of crystallization values. The shift of around 12–15 °C for crystallization peak can be observed for the nanocomposite fibers.

Integration of the exothermic peak the non-isothermal crystallization can give the relative degree of crystallinity as function time. Figure 14.7 shows the normalized graph of relative crystallinity *% vs.* time for nylon-6 and nanocomposite samples (replica 1). Though nucleation occurs earlier the crystals in nanocomposites grow very slowly compared with the neat nylon-6 sample.

The Avrami equation was used to analyze the non-isothermal crystallization process.[18] Figure 14.8 shows the plot of ln $[-\ln(1 - X_t)]$ *vs.* ln $t$ to describe the non-isothermal crystallization process. Non-isothermal crystallization parameters, Avrami exponent $n$ and rate constant $k$, were determined from the slope and the interception of the best fit.

Table 14.4 shows the values of half-crystallization time and Avrami exponent $n$ and rate constant $k$. The values of $n$ around 1.4–1.5 suggest the rod-shaped crystal geometry and thermal nucleation type.[17] Results show that rate constant $k$ has been significantly changed due to inclusion of the carbon nanotubes. This suggests that carbon nanotubes restrict or interfere with the growth of the crystals that are around the vicinity of the carbon nanotubes.

### 14.4.3 Molecular weight

Neat nylon-6 and nanocomposite samples were characterized using dilute solution viscometry to understand the effect of carbon nanotubes on the

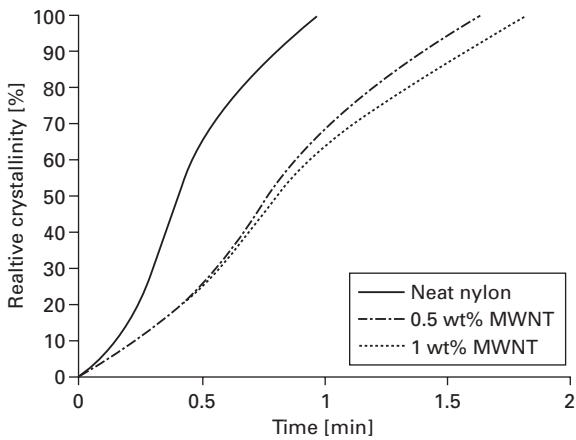


*14.7* Effect of carbon nanotubes on crystal growth.

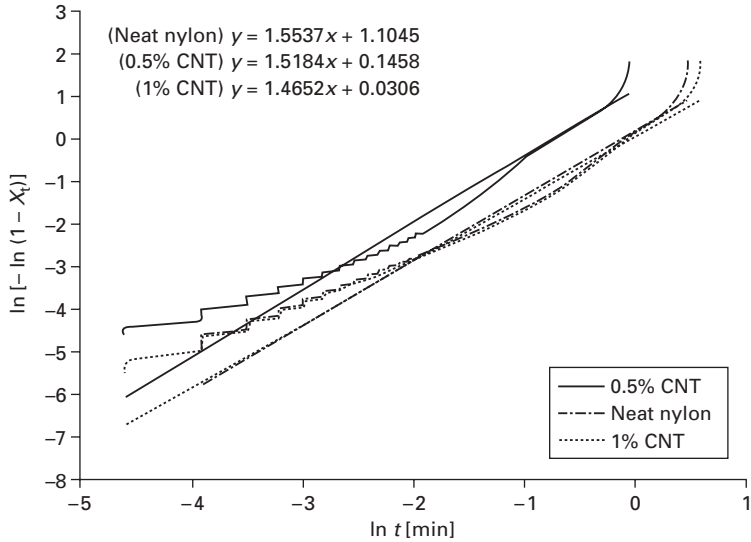


*14.8* Determination of Avrami parameters.

*Table 14.4* Avrami parameters for neat nylon-6 and nanocomposite

| | $t_{1/2}$ Crystallization half-time (min) | Avrami parameters | |
|---|---|---|---|
| | | $K$ (min$^{-1}$) | $n$ |
| Neat nylon | 0.420 | 1.054 | 1.548 |
| 0.5 wt% MWNT | 0.760 | 0.176 | 1.497 |
| 1 wt% MWNT | 0.825 | 0.039 | 1.454 |

molecular weight of the nylon-6 polymer synthesized. Figure 14.9 shows the plots of the reduced and inherent viscosities *vs*. concentrations. The observation of the graphs shows that nanocomposite samples, even though they were expected to show higher intrinsic viscosities because of the presence of carbon nanotubes, have lower intrinsic viscosities. Therefore it can be concluded that the nanocomposites have lower molecular weights than the neat nylon-6 polymer. Equation 14.2 was used to determine the intrinsic viscosities for the nanocomposite samples excluding the effect of the carbon nanotubes on the viscosity. The length of the carbon nanotubes was assumed to be 4 µm. The volume fraction for the 0.5 wt% and 1 wt% MWNTs on weight of polymers was determined to be 0.004 and 0.008. The diameter of the used MWNTs was 30 nm. Table 14.5 shows the average intrinsic viscosities for neat nylon-6 and nanocomposite samples after excluding the effect of carbon nanotubes on viscosity.

The molecular weights for neat nylon-6 polymer and nanocomposite samples were then calculated using the Mark–Houwink equation (Table 14.6). The

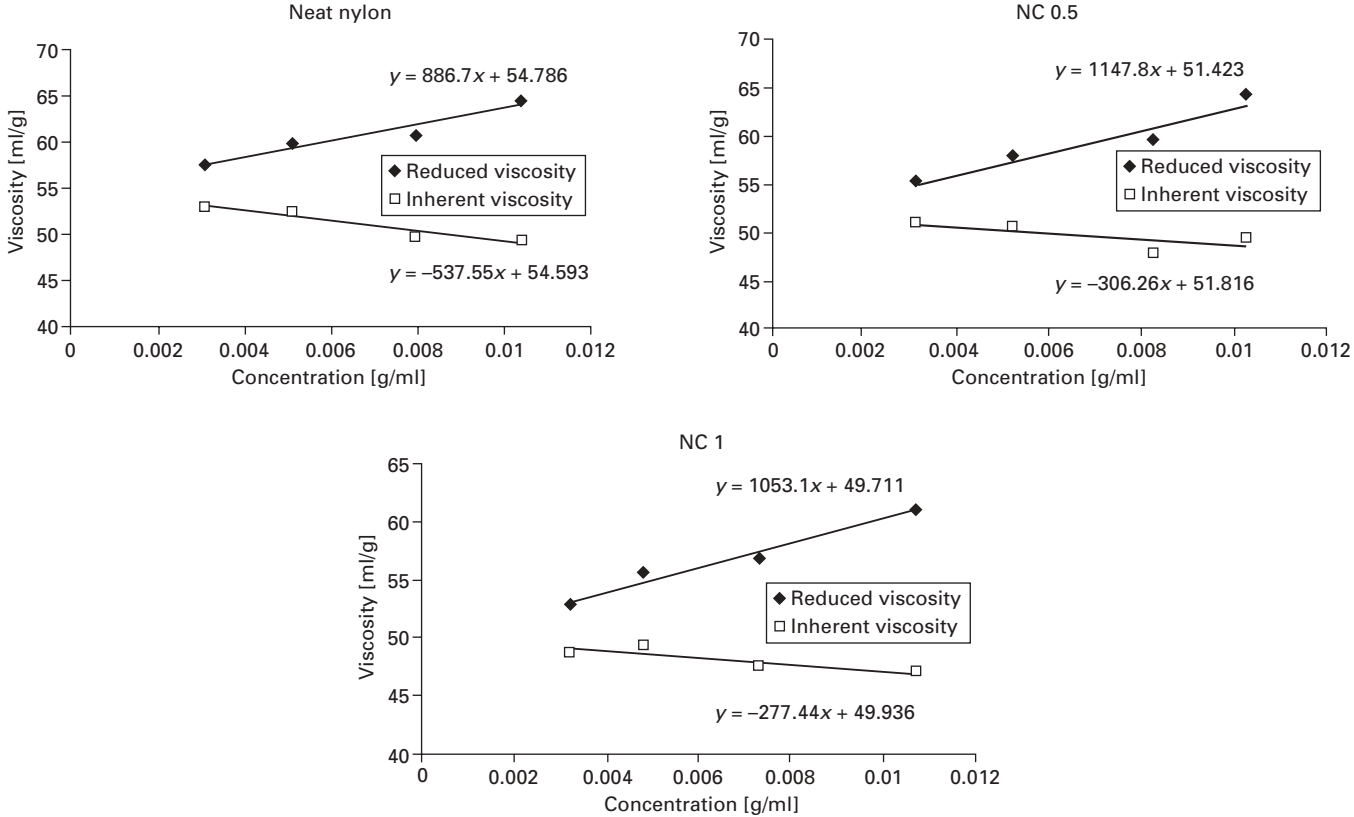


*14.9* Determination of the intrinsic viscosity for neat nylon and nanocomposite samples.

*Table 14.5* Intrinsic viscosities for the neat nylon and nanocomposite samples after application of Equation 14.2

| | Intrinsic viscosity (ml/g) | | |
|---|---|---|---|
| | Replica 1 | Replica 2 | Average |
| Neat nylon | 54 | 55 | 54 |
| NC 0.5 | 51 | 52 | 51 |
| NC 1 | 48 | 50 | 49 |

*Table 14.6* Determination of molecular weights using the Mark–Houwink equation

| | Intrinsic viscosity (ml/g) | $M_v$ (g/mol) |
|---|---|---|
| Neat nylon | 54 | 19700 |
| NC 0.5 | 49 | 17100 |
| NC 1 | 45 | 15100 |

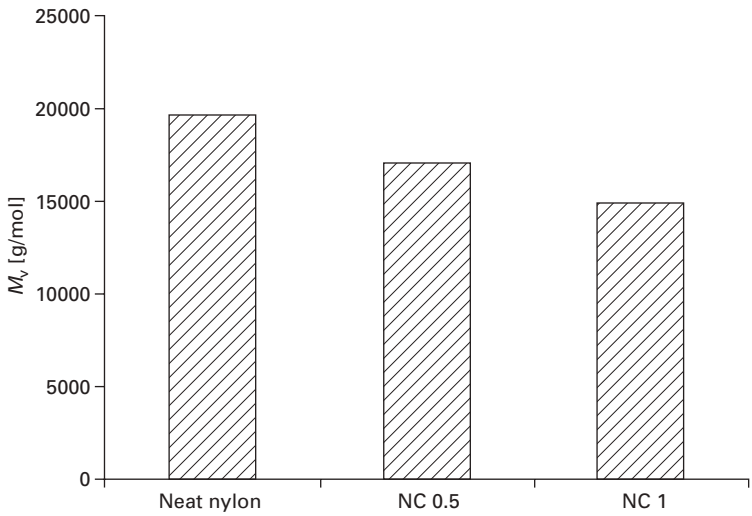


*14.10* Viscosity average molecular weights for neat nylon-6 polymer and nanocomposite samples.

viscosity average molecular weight ($M_v$) was significantly reduced by the addition of carbon nanotubes; $M_v$ decreased by about 13% with 0.5 wt% addition of MWNTs and by about 23% with the 1 wt% addition of MWNTs. Figure 14.10 graphically represents the affect of carbon nanotubes on the molecular weight. Results of dilute solution viscometry thus confirm the conclusions made in Section 14.2. The carbon nanotubes lower the rate of

polymerization. This decreased polymerization rate results in activation of more and more initiator molecules resulting in lowering of the molecular weight.

### 14.4.4 Tensile properties

Table 14.7 shows average mechanical properties for nylon-6 and nanocomposite fibers. It also shows the standard deviation for the modulus, strength and breaking strain values. All the samples showed high variability in properties. Variability was higher in the case of nanocomposite samples. The reasons behind the high variability can be attributed to the absence of deaeration, mixing of the purging compound and localized MWNT agglomerates in the case of nanocomposites.

The initial moduli for neat nylon-6 and nanocomposite samples are compared in Fig. 14.11. The initial modulus increased with draw ratio for all the samples. Increase in initial modulus was observed for nanocomposite samples compared with neat nylon samples. The nanocomposite sample with 0.5 wt% MWNTs stretched four times shows the highest initial modulus. Nanocomposite samples with 1 wt% MWNTs show lower initial modulus values compared with samples with 0.5 wt% MWNT but they show higher values than those of the neat nylon-6 sample. This is a result of the lowered molecular weight in the case of 1 wt% MWNTs nanocomposite compared with 0.5 wt% MWNTs nanocomposite.

The breaking strengths of neat nylon-6 and nanocomposite samples are compared in Fig. 14.12. Increase in the strength was observed for the nanocomposite samples. The highest strength value was observed for the

*Table 14.7* Average mechanical properties for nylon-6 and nanocomposite fibers

| | Neat nylon DR-3 | Neat nylon DR-4 | NC 0.5 DR-3 | NC 0.5 DR-4 | NC 1 DR-3 | NC 1 DR-4 |
|---|---|---|---|---|---|---|
| Modulus (MPa) | 1149 | 1302 | 1553 | 1837 | 1353 | 1641 |
| SD modulus (MPa) | 96 | 112 | 189 | 258 | 118 | 169 |
| Strength (MPa) | 205 | 224 | 261 | 327 | 226 | 277 |
| SD strength (MPa) | 12 | 10 | 29 | 30 | 20 | 34 |
| Breaking strain (%) | 33 | 24 | 39 | 23 | 38 | 17 |
| SD breaking strain (%) | 6 | 5 | 7 | 4 | 7 | 3 |

DR draw ratio, NC 0.5 nanocomposite with 0.5 wt% MWNTs, NC 1 nanocomposite with 1 wt% MWNTs, SD standard deviation.

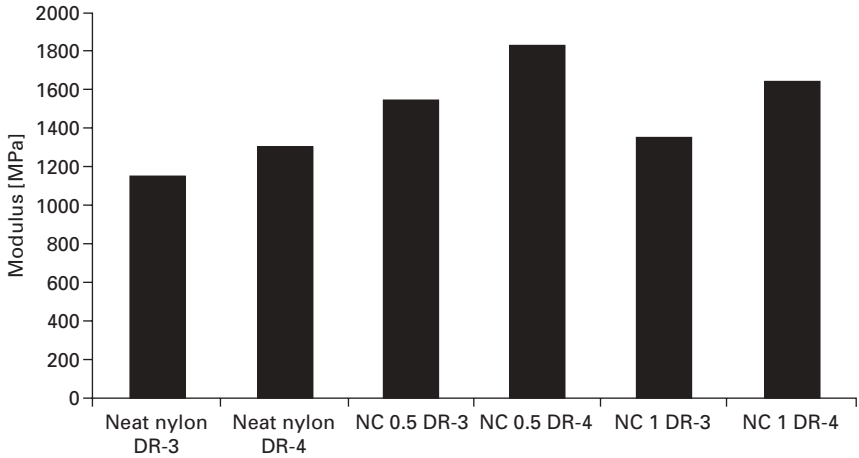


*14.11* Comparison of moduli of nylon-6 and nanocomposite samples.

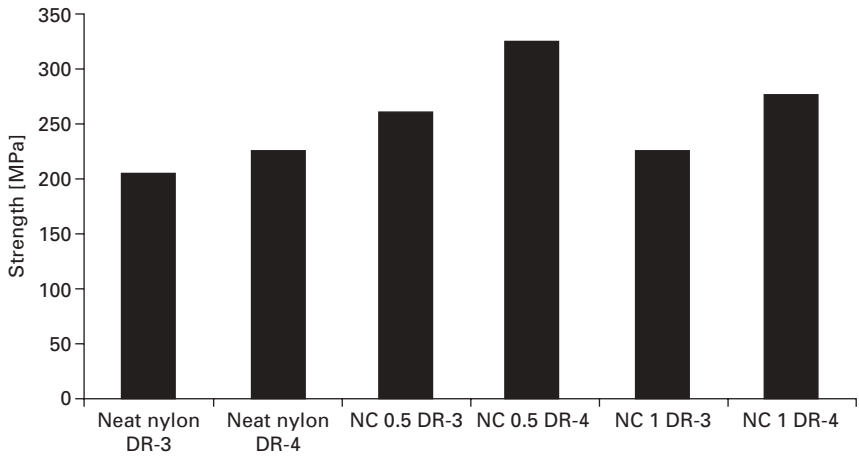


*14.12* Comparison of strengths of nylon-6 and nanocomposite samples.

nanocomposite sample with 0.5 wt% MWNTs stretched four times; however, nanocomposite samples with 1 wt% MWNTs show lower strength values compared with samples with 0.5 wt% MWNT but higher values than those of the neat nylon-6 sample. This is a result of the lowered molecular weight in the case of 1 wt% MWNTs nanocomposite compared with 0.5 wt% MWNTs nanocomposite. A somewhat unusual trend can be observed for the strain-at-break values for neat nylon-6 and nanocomposite samples (Fig. 14.13). Higher breaking strain values were observed in the case of nanocomposite samples that were stretched three times. But after stretching four times, breaking

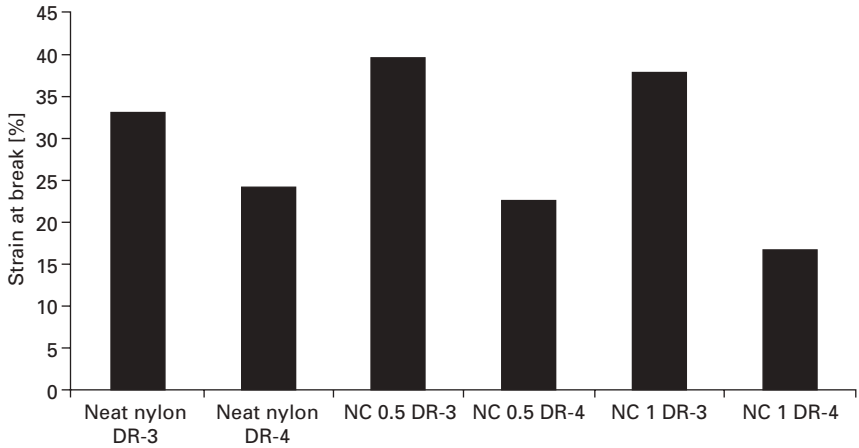


*14.13* Comparison of strains at break of nylon-6 and nanocomposite samples.

*Table 14.8* Percentage change in mechanical properties of nanocomposite samples compared with neat nylon-6 samples

| | | Change (%) | | | |
|---|---|---|---|---|---|
| | | NC 0.5 DR-3 | NC 0.5 DR-4 | NC 1 DR-3 | NC 1 DR-4 |
| Modulus | Neat nylon DR-3 | +35 | | +18 | |
| | Neat nylon DR-4 | | +41 | | +26 |
| Strength | Neat nylon DR-3 | +27 | | +10 | |
| | Neat nylon DR-4 | | +46 | | +24 |
| Strain % at break | Neat nylon DR-3 | +19 | | +14 | |
| | Neat nylon DR-4 | | –7 | | –31 |

strain values go down drastically and are lower than those of neat nylon-6 samples stretched four times.

Table 14.8 shows the percentage change in mechanical properties due to reinforcement of the carbon nanotubes in neat nylon-6. The maximum increase of 41% and 46% in modulus and strength respectively was observed in the case of nanocomposites with 0.5 wt% MWNT stretched four times. Less improvement can be observed in the case of nanocomposites with 1 wt% MWNT, likely due to the lower molecular weight of the nylon.

Table 14.9 shows the effect of drawing on the percentage change in mechanical properties of the neat nylon-6 and nanocomposite samples. Results show that percentage improvements are higher in nanocomposite samples compared with neat nylon-6 samples when samples were further stretched from three to four times. For example, when neat nylon-6 samples were

*Table 14.9* Effect of draw ratio on percentage change in mechanical properties of nanocomposite and neat nylon-6 samples

| | | Change (%) | | |
|---|---|---|---|---|
| | | Neat nylon DR-4 | NC 0.5 DR-4 | NC 1 DR-4 |
| Modulus | Neat nylon DR-3 | +13 | | |
| | NC 0.5 DR-3 | | +18 | |
| | NC 1 DR-3 | | | +21 |
| Strength | Neat nylon DR-3 | +9 | | |
| | NC 0.5 DR-3 | | +25 | |
| | NC 1 DR-3 | | | +23 |
| Strain % at break | Neat nylon DR-3 | –27 | | |
| | NC 0.5 DR-3 | | –43 | |
| | NC 1 DR-3 | | | –56 |

*Table 14.10* Change in mechanical properties of nanocomposite samples (0.5 wt% and 1 wt% MWNT)

| | | Change (%) | |
|---|---|---|---|
| | | NC 1 DR-3 | NC 1 DR-4 |
| Modulus | NC 0.5 DR-3 | –13 | |
| | NC 0.5 DR-4 | | –11 |
| Strength | NC 0.5 DR-3 | –14 | |
| | NC 0.5 DR-4 | | –15 |
| Strain % at break | NC 0.5 DR-3 | –4 | |
| | NC 0.5 DR-4 | | –26 |

further stretched from three to four times, modulus increased by 13%. On the other hand, 18 and 21% improvements can be observed in the case of 0.5 wt% and 1 wt% MWNT respectively. Similar results can be observed in the case of strength values. This must be a result of orientation of carbon nanotubes along the fiber axis when samples were further stretched from three to four times. Table 14.10 shows the comparison of mechanical properties between nanocomposite samples with 0.5 wt% MWNT and 1 wt% MWNT. All the properties decreased with further addition of carbon nanotubes. This can be possibly be attributed to the reduction of molecular weight in the case of the 1 wt% MWNT nanocomposite sample compared with the 0.5 wt% MWNT sample.

## 14.5 Conclusions

Nylon-6/MWNT nanocomposites were prepared by an *in situ* polymerization technique. Different studies were done on the nylon-6/MWNT nanocomposites

and extruded nanocomposite fibers and the following conclusions were made:

- Nanocomposites with more than 1 or 1.5 wt% MWNTs could not be prepared by the proposed technique due to reduced polymerization rate. If the reaction were carried out for a longer time then polymerization failed either due to the reaction of the monomer mixture with moisture in the air or degradation of the chemicals due to heating for the longer duration.
- SEM analysis of the cross-section of the stretched and broken nanocomposite fibers showed that carbon nanotubes were well separated in the polymer matrix. Carbon nanotubes also appeared to be nearly oriented along the direction of the fiber axis due to the effect of the extrusion and stretching.
- Crystallization kinetics study using DSC indicated that although carbon nanotubes acted as a nucleating agent at the initial stage, they significantly lowered the crystallization rate or crystal growth.
- Dilute solution viscometry study showed that nylon-6 polymer in the nanocomposites has a lower molecular weight than that of neat nylon-6 polymer polymerized with same concentration of the initiator. Viscosity average molecular weight decreased from 19 700 to 17 100 g/mol for 0.5 wt% addition of the MWNTs and to 15 100 g/mol for 1 wt% addition of the MWNTs due to restricted chain growth.
- Tensile testing of neat nylon-6 and nanocomposite fibers showed that reinforcement of nylon-6 fiber by carbon nanotubes increased the modulus and the strength of the fibers significantly (95% confidence level). Compared with neat nylon fibers, maximum improvements (41% in modulus and 46% in strength) were observed for the 0.5 wt% MWNT nanocomposite fibers that were stretched four times. But improvements were reduced to 26% in modulus and 23% in strength for the 1 wt% MWNT nanocomposite fibers, stretched four times, possibly due to the reduced molecular weight (23%). The results further showed that additional stretching of the fibers from three to four times, possibly further oriented the carbon nanotubes and resulted in additional improvements in modulus and strength.

## 14.6 Acknowledgments

The authors would like to express their gratitude to Mr Leo Barish for his help and discussions in microscopy. Thanks are given to Professor Steve Warner for his suggestions. The authors acknowledge Hyperion Catalysis for providing us with multiwall nanotubes and Honeywell for supplying the nylon-6. Finally authors are grateful to the National Textile Center (NTC) for funding this project under Department of Commerce grant no. 0207400.

## 14.7 References


1. Iijima, S., *Nature*, London, **56**, pp 354, 1991
2. Satio, R., Dresselhaus, G., Dresselhaus, M., *Physical Properties of the Carbon Nanotubes*, Imperial College Press, London, 1998
3. Harris, P., *Carbon Nanotubes and Related Structures: New Materials for the 21st Century*, Cambridge University Press, New York, 1999
4. Pan, Z., Xie, S., Lu, L., Chang, B., Sun, L., *Applied Physics Letters*, **74**, pp 3152–3154, 1999
5. Qian, D., Dickey, E., Andrews, R., *Applied Physics Letters*, **76**, pp 2868–2870, 2000
6. Thess, A., Lee, R., Nikolaev, P., Dia, H., Petit, P., *Science*, **273**, pp 483–487, 1996
7. Journet, C., Maser, W., Bernier, P., Loiseau, A., De La Chapelle, M., *Nature*, **388**, pp 756–758, 1997
8. Tans, S.J., *et al*., *Nature*, **393**, p 49, 1998
9. Wei, B.Q., *et al.*, *Applied Physics Letters*, **79**, p 1172, 2001
10. Hone, J., *Topics In Applied Physics*, **80**, p 273, 2001
11. Collins, P. Avouris, Ph., *Scientific American*, No. 12, p 62, 2000
12. Ajayan, P., Schadler, L., Giannaris, C., Rubio, A., *Advanced Materials*, **12**(10), pp 750–753, 2000
13. Brandrup, J., Immergut, E.H., *Polymer Handbook*, 3rd edn, Wiley, New York, 1989
14. Kirkwood, J.G., Auer, P.L., *Journal of Chemical Physics*, **19**, pp 281–283, 1951
15. Davis, V.A., *et al*., *Macromolecules*, **37**, pp 154–160, 2004
16. Sandler J., Shaffer, M.S.P., Prasse, T., Bauhofer, W., Schulte, K., *Polymer*, **40**, pp 5967–5971, 1999
17. Hiemenz, P.C., *Polymer Chemistry: The Basic Concepts*, Marcel Dekker, New York, 1984
18. Li, Y., Zhang, G., Zhu, X., Yan, D., *Journal of Applied Polymer Science*, **88**, pp 1311–1319, 2000